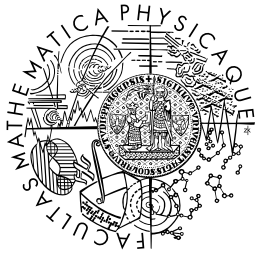

FACULTY
OF MATHEMATICS
AND PHYSICS
Charles University

MASTER THESIS

Bc. Jiří Malík

Thermomechanical interaction between outer ice shells and deep oceans on icy moons of Jupiter and Saturn

Mathematical Institute of Charles University

Supervisor of the master thesis:	RNDr. Ondřej Souček, Ph.D.
Study programme:	Mathematics
Study branch:	Mathematical Modelling in Physics and Technology

Prague 2018

I declare that I carried out this master thesis independently, and only with the cited sources, literature and other professional sources.

I understand that my work relates to the rights and obligations under the Act No. 121/2000 Sb., the Copyright Act, as amended, in particular the fact that the Charles University has the right to conclude a license agreement on the use of this work as a school work pursuant to Section 60 subsection 1 of the Copyright Act.

In ..... date ..... signature of the author

Title: Thermomechanical interaction between outer ice shells and deep oceans on icy moons of Jupiter and Saturn

Author: Bc. Jiří Malík

Institute: Mathematical Institute of Charles University

Supervisor: RNDr. Ondřej Souček, Ph.D., Mathematical Institute of Charles University

Abstract: The thesis contains a survey of numerical tools for studying thermomechanical interactions of a two-phase system contained in a domain with an upper boundary that forms a free surface. The enthalpy diffused-interface formulation is used for an approximation of the phase change interface and the computing algorithm is benchmarked against an analytical solution of the Stefan problem. Arbitrary Lagrangian-Eulerian kinematical description of the continuum is applied to overcome the difficulty in the form of the free surface. The validity of the approach is examined on a thermal convection benchmark problem.

Keywords: icy moons of Jupiter and Saturn, viscous deformation, free surface problem, Stefan problem, finite element method

I am very pleased that I can hereby express my gratitude to my parents without whose support I would not even imagine this academic journey. Thank you.

I am deeply indebted to my supervisor Ondřej Souček who was not only able to point me in the right direction but also helped me to walk in it.

Contents

List of Symbols and Abbreviations

Symbols – in order of appereance

$\omega(t)$	domain
$\sigma(t)$	singular surface
$\gamma_{\mathrm{f}}(t)$	free surface
$a^{\mathrm{s}},\ a^{\mathrm{l}}$	value of quantity a pertaining to solid, liquid phase
$\gamma_{\mathrm{f}}(t)$	free surface
$\mathbf{n}_\sigma$	unit normal of singular surface
$\mathbf{v}$	Eulerian particle velocity field
$\mathbf{w}$	Eulerian interface velocity field
ρ	(mass) density
$\mathbf{t}$	surface traction
$\mathbf{b}$	body force density
$\mathbb{T}$	Cauchy stress tensor
$\mathbb{I}$	identity tensor
e	internal energy density
$\mathbf{q}$	heat flux
b_e	heat supply density
$\mathbb{D}$	symmetric part of velocity gradient, $\mathbb{D} \coloneqq \frac{1}{2}\left(\nabla\mathbf{v} + (\nabla\mathbf{v})^T\right)$
E	total energy density
η	entropy density
b_η	entropy source density
$\mathbf{q}_\eta$	entropy flux
p^{th}	thermodynamic pressure
θ	thermodynamic temperature
h	enthalpy density
c_p	molar heat capacity at constant pressure
β_{V}	thermal expansion coefficient
m	mean normal stress
$\mathbb{A}^\delta$	deviatoric part of tensor $\mathbb{A}$, $\mathbb{A}^\delta \coloneqq \mathbb{A} - \frac{1}{3}\operatorname{Tr}\mathbb{A}$
$\mathbb{S}$	shear part of Cauchy stress tensor
L	latent heat of fusion
L_{m}	latent heat of melting
θ_{m}	melting temperature
$\chi_{(a,b)}(x)$	characteristic function of interval (a, b)
ϵ	mollifying parameter
f_ϵ	mollification of quantity f
μ	dynamic viscosity
k	thermal conductivity
$H(x), H^0_\epsilon(x)$	Heavyside step function, jump at $x = 0$, C^0 approximation
$\delta(x), \delta^0_\epsilon(x)$	Dirac delta distribution, center at $x = 0$, C^0 approximation
$C_k,\ k \in \mathbb{N}_0$	integration constants

Abbreviations – in alphabetical order

ALE	Arbitrary Eulerian-Lagrangean
ASI	Italian Space Agency
CFD	Computational fluid dynamics
CFL	Courant-Friedrichs-Lewy (condition)
ESA	European Space Agency
FEM	Finite Element Method
NASA	National Aeronautics and Space Administration
ODE	Ordinary differential equation
PDE	Partial differential equation

Introduction

A very successful Cassini-Huygens space mission was able to explore a possibly life harbouring planetary object within our Solar system. This relatively small icy moon, called Enceladus, has the necessary conditions for life—heat and liquid water. Contrary to expectations, the moon is still very active and its silicate core, whose particles were detected by the Cassini spacecraft, contains heat sources. A model of thermomechanical interaction between outer ice shells and deep oceans on long time scales might contribute to an overall understanding of the moon's evolution. Such a question is remarkably important in the context of a possible presence of any form of life. This thesis only gives a simple formulation of the thermomechanical problem connected with the important question above, it studies mathematical difficulties of the formulation and proposes suitable tools for their solution.

The first complication is connected with the phase transition within the domain. The melting front represents an abrupt change of material properties. Such a change may be very inconvenient from the computational point of view. An approximation of the melting front is a possible solution. Thus we come at the so called diffused-interface formulation. Thermomechanical description of the domain is given by the enthalpy potential. Enthalpy method is an application of the diffused-interface formulation on our problem. Chapter 1 provides mathematical formulation of the problem and derives the enthalpy method for the problem.

Stefan problem and its anaytical solution provides a solid background for benchmarking of the enthalpy method. Formulation and analytical solution of the Stefan problem in one, two and three spatial dimensions are presented in Chapter 2. The chapter is completed with result comparison for one-dimensional and two-dimensional cylindrically symmetric Stefan problem. A small remark on the stability of the one-dimensional numerical algorithm is attached. To our knowledge, benchmarking of the Stefan problem in two spatial dimensions is new.

The surface of the moon is not a subject to any traction, therefore it formes the so called free surface. Our domain, that describes the cross section of the planetary body, is thus time-dependent. The tool described in Chapter 3 provides a kinematical description that is well-suited for problems with the free surface. The arbitrary Lagrangian-Eulerian description is applied on the Earth's mantle convection benchmark problem and results for the fixed domain and the free surface formulation are compared.

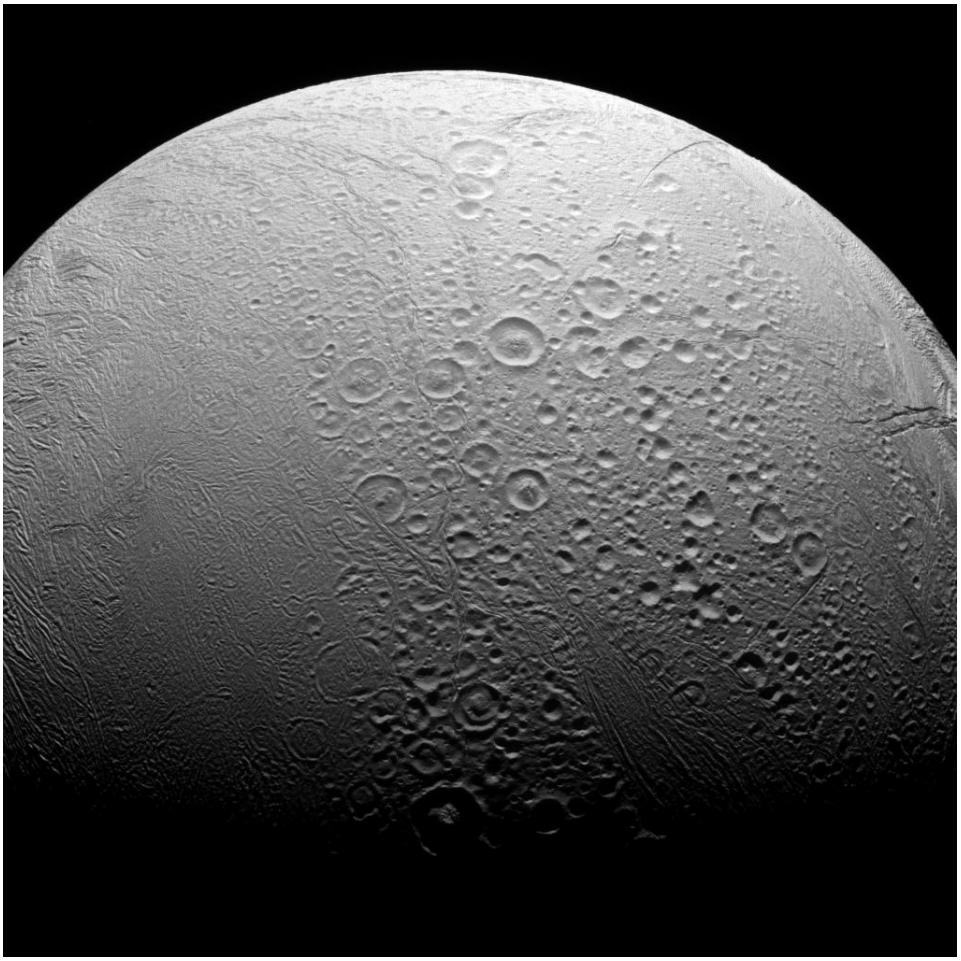

source: https://saturn.jpl.nasa.gov/

1. Problem formulation

1.1 Motivation

In 1997 began a journey to what was originally intended to be a four year mission, but it lasted almost a decade longer. The Cassini-Huygens[i] mission was the collaborative effort of three space agencies (NASA, ESA and ASI—Italian Space Agency). It ended in 2017 and brought a vast amount of data about several planetary bodies of our Solar system. For more information about the mission, the reader can visit https://saturn.jpl.nasa.gov/.

Enceladus, an icy moon of the planet Saturn, quickly became a point of interest of astrobiologists, since both liquid water and heat sources are present beneath the icy shell. The relatively small body with the radius of 252 kilometers provides conditions hospitable to life.

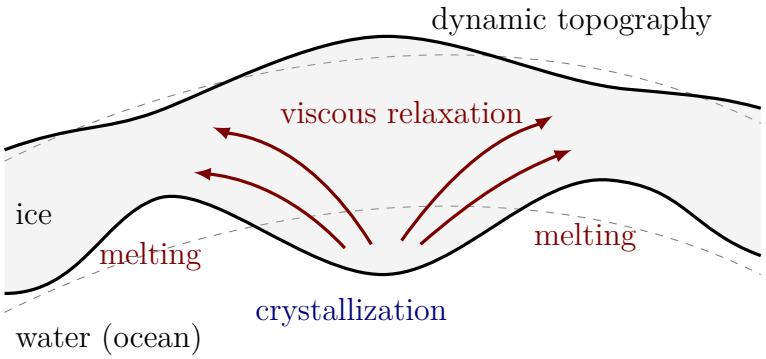

Figure 1.1: Main mechanisms of thermomechanical interaction between the icy shell and the heated water.

Ongoing research has shown that Enceladus is still geologically very active icy moon, which is indicated by a presence of water vapor plumes on the south pole of the mentioned satellite. The material escaping through these plumes is a source of the Saturn's E ring. The high heat fluxes connected with the vapor plumes can be explained by the localised solid-state convection of ice. The total picture of the main themomechanical processes taking place in the ice crust and on its interface with the ocean depicted in Figure 1.1 is completed by the fact that Enceladus is one of the brightest object in the Solar system. It has the albedo of approximately 80%, thus it reflects the majority of incoming radiation. Other general information about Enceladus can be found in [Spencer and Nimmo, 2013].

According to [Beuthe, 2018], the average thickness of the ice crust can be approximated by spherical harmonics of low degrees which reads:

$$d = d_{00} + d_{20} P_{20}(\cos(\pi/2 - \phi)) + d_{22} P_{22}(\cos(\pi/2 - \phi)) \cos 2\varphi + d_{30} P_{30}(\cos(\pi/2 - \phi)),$$

[i] Giovanni Domenico **Cassini** (1625–1712) – Italian mathematician and astronomer, he was the first to observe that Saturn's rings (which were discovered by Galileo) are divided.

Christiaan **Huygens** (1629–1695) – Dutch physicist and astronomer, also a very creative inventor (patented pendulum clock), who among others studied Saturn's rings.

where $(d_{00}, d_{20}, d_{22}, d_{30}) = (22.8, -12.1, 1.3, 3.7) \pm (4, 2.4, 0.3, 0.7)\,\mathrm{km}$ and P_{nm} are the unnormalised Legendre polynomials associated to the spherical harmonics, ϕ is the latitude and φ is the longitude. The only basis function that lacks radial symmetry is P_{22} and it is weighted with the smallest coefficient d_{22}. Consequently (and in accordance with Beuthe) we will ignore the longitudinal thickness variations. This enables us to exploit the two-dimensional nature of the problem and preferably present only the planar formulation.

1.2 Mathematical model

Main objective of this section is to provide a general mathematical and physical framework for a formulation of the problem.

1.2.1 Geometry and boundary conditions

Our domain of interest constists of a part of the cross section of the whole planetary body (see Figure 1.2). In our abstraction this domain contains the two discernible phases denoted by $\omega_\mathrm{l}(t)$ for liquid water and $\omega_\mathrm{s}(t)$ for solid (ice) phase, respectively.

The subregions are divided by a smooth singular surface denoted by $\sigma(t)$, whose well-defined normal $\mathbf{n}_\sigma$ is oriented *into* the solid phase subregion. For the future purposes we will take $\omega := \omega_\mathrm{l} \cup \omega_\mathrm{s} \cup \sigma$ to be the domain containing the both phases along with the singular surface.

Our model describes the top boundary γ_f as the free surface, thus the domain ω is time-dependent. Having in mind that the geometry represents only part of the bigger system, we equip its side walls γ_p with periodic boundary conditions. The bottom boundary γ_0 represents a border of a porous core. We expect that the fluid phase is able to slip freely on this boundary.

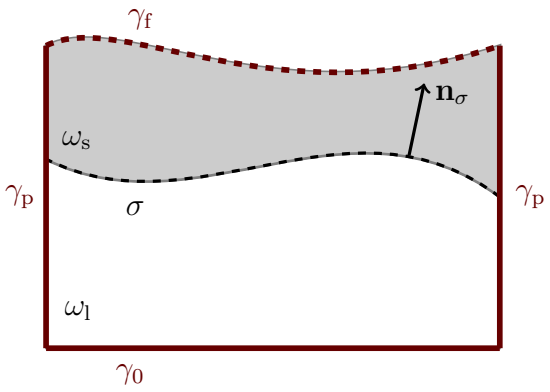

Figure 1.2: Geometrical description of the domain of interest.

In comparison with the usual continuum mechanics problems, our formulation needs to consider the two folloiwng difficulties:

- the phase change interface—represented by the singular surface $\sigma(t)$
- the free surface $\gamma_\mathrm{f}(t)$.

For both of these hindrances, we will propose a possible method together with its validation in the form of a benchmark comparison.

Thermomechanical interactions of the phases are described by a system of PDEs, called *balance laws*. These balance laws (or simply balances) can be expressed in an integral form using generalisations of two important results from vector calculus:

The *Divergence Theorem* for a vector field $\mathbf{h}$ applied to the time-dependent domain $\omega(t)$, that experiences a discontinuity across the singular surface $\sigma(t)$ but $\mathbf{h}$ is continuously differentiable inside $\omega(t)\backslash\sigma(t)$, for every t[ii]:

$$\int_{\omega(t)} \mathbf{h}\cdot\mathbf{n}_\sigma \,\mathrm{d}a = \int_{\omega(t)\backslash\sigma(t)} \operatorname{div}\mathbf{h}\,\mathrm{d}v + \int_{\sigma(t)} [\![\mathbf{h}]\!]\cdot\mathbf{n}_\sigma \,\mathrm{d}a, \tag{1.1}$$

where $[\![\mathbf{h}]\!] \coloneqq \mathbf{h}^+ - \mathbf{h}^-$ denotes the jump of the vector field $\mathbf{h}$ across the singular surface $\sigma(t)$, i.e.:

$$\begin{aligned}\forall t, \forall \mathbf{x}\in\sigma(t) : \mathbf{h}^+(t,\mathbf{x}) &\coloneqq \lim_{s\to 0^+} \mathbf{h}(t,\mathbf{x}+s\mathbf{n}_\sigma(t,\mathbf{x})),\\ \mathbf{h}^-(t,\mathbf{x}) &\coloneqq \lim_{s\to 0^-} \mathbf{h}(t,\mathbf{x}+s\mathbf{n}_\sigma(t,\mathbf{x})).\end{aligned}$$

Using the previous result, the generalised *Reynolds' Transport Theorem* for a scalar field f, that is continuously differentiable inside $\omega(t)\backslash\sigma(t)$, can be expressed as follows:

$$\frac{\mathrm{D}}{\mathrm{D}t}\int_{\Omega(t)} f\,\mathrm{d}v = \int_{\omega(t)\backslash\sigma(t)} \left[\frac{\partial f}{\partial t} + \operatorname{div}(f\mathbf{v})\right]\mathrm{d}v + \int_{\sigma(t)} [\![f(\mathbf{v}-\mathbf{w})]\!]\cdot\mathbf{n}_\sigma\,\mathrm{d}a, \tag{1.2}$$

where $\mathrm{D}/\mathrm{D}t \coloneqq \partial/\partial t + (\mathbf{v}\cdot\nabla) = \partial/\partial t + v_i\partial/\partial x_i$ denotes the material (or substantial) derivative. We also need to distinguish between the particle velocity $\mathbf{v}$ and $\mathbf{w}$[iii], the velocity of the interface (represented by the singular surface $\sigma(t)$), which are not generally equal. The same result, with minor changes in notation, holds true for vector and tensor variables. For proofs of both theorems, see [Hutter and Jöhnk, 2010], subsection 3.2.1.

1.2.2 Balance laws and governing equations

Present subsection contains formulation of the fundamental principles of the continuum mechanics, viz. balance laws. These laws are given in a global (or integral) form for a body of the continuum containing the singular surface $\sigma(t)$. Notation and formulations of the laws are similar to those presented in lecture notes [Martinec, 2003].

Physical properties of the body are given by the postulated densities of physical variables. Under the additive assumption we can integrate those densities

[ii] Notation convention that is being used in the thesis can be found in Appendix A: Notation

[iii] We do not consider cracks to occur, this implies:

$$[\![\mathbf{w}]\!]\cdot\mathbf{n}_\sigma = 0, \tag{1.3}$$

which does not necessarily mean that $\mathbf{w}$ is continous on $\omega(t)$, its tangential part is, nevertheless, physically irrelevant.

over infinitesimal volume elements to obtain the physical property of the whole body. If we moreover suppose that the balance laws hold for any part of the body (assumptions of the local continuum mechanics), we can derive field equations (or differential form of balance laws) characterising physical variables locally.

Conservation of mass and continuity equation

Employing the previous formulae, we can express the integral form of the *Law of Mass Conservation*:

$$\frac{\mathrm{D}}{\mathrm{D}t}\int_{\omega(t)}\rho\,\mathrm{d}v \overset{(1.2)}{=} \int_{\omega(t)\setminus\sigma(t)}\left[\frac{\partial\rho}{\partial t}+\operatorname{div}(\rho\mathbf{v})\right]\mathrm{d}v+\int_{\sigma(t)}[\![\rho\,(\mathbf{v}-\mathbf{w})]\!]\cdot\mathbf{n}_\sigma\,\mathrm{d}a=0, \quad (1.4)$$

where ρ is the (mass) density of the material. Under the postulate that the mass balance law is valid for an arbitrary part of the volume $\omega(t)$ and the singular surface $\sigma(t)$, we can deduce that both of the integrands in the integral mass balance law (1.4) are identically zero. We thus come to the so-called *continuity equation*, complemented by a jump of the density across the singular surface $\sigma(t)$:

$$\frac{\mathrm{D}\rho}{\mathrm{D}t}=-\rho\operatorname{div}\mathbf{v} \quad \text{in } \omega(t)\setminus\sigma(t), \quad (1.5)$$

$$[\![\rho\,(\mathbf{v}-\mathbf{w})]\!]\cdot\mathbf{n}_\sigma=0 \quad \text{on } \sigma(t). \quad (1.6)$$

Balance of linear momentum and equations of motion

Another fundamental balance law is that of *(linear) momentum*. Let us assume that the body is a subject to surface traction $\mathbf{t}(\mathbf{n})$, that depends on the surface normal $\mathbf{n}$, and a resultant of the body forces $\rho\mathbf{b}$. Application of the *Cauchy Lemma*[iv] yields:

$$\begin{aligned}\frac{\mathrm{D}}{\mathrm{D}t}\int_{\omega(t)}\rho\mathbf{v}\,\mathrm{d}v &= \oint_{\partial\omega(t)}\mathbf{t}(\mathbf{n})\,\mathrm{d}a+\int_{\omega(t)}\rho\mathbf{b}\,\mathrm{d}v=\\ &=\oint_{\partial\omega(t)}\mathbb{T}\mathbf{n}\,\mathrm{d}a+\int_{\omega(t)}\rho\mathbf{b}\,\mathrm{d}v=\\ &\overset{(1.1)}{=}\int_{\omega(t)\setminus\sigma(t)}\operatorname{div}\mathbb{T}+\rho\mathbf{b}\,\mathrm{d}v+\int_{\sigma(t)}[\![\mathbb{T}]\!]\mathbf{n}_\sigma\,\mathrm{d}a, \quad (1.7)\end{aligned}$$

$$\begin{aligned}\frac{\mathrm{D}}{\mathrm{D}t}\int_{\omega(t)}\rho\mathbf{v}\,\mathrm{d}v \overset{(1.2)}{=}&\int_{\omega(t)\setminus\sigma(t)}\left[\frac{\partial(\rho\mathbf{v})}{\partial t}+\operatorname{div}(\rho\mathbf{v}\otimes\mathbf{v})\right]\mathrm{d}v+\\ &+\int_{\sigma(t)}[\![\rho\mathbf{v}\otimes(\mathbf{v}-\mathbf{w})]\!]\mathbf{n}_\sigma\,\mathrm{d}a, \quad (1.8)\end{aligned}$$

where $\mathbb{T}$ denotes the Cauchy stress tensor, i.e. $\operatorname{div}\mathbb{T}$ represents the action of surface forces on the volume element $\mathrm{d}v$ and $\mathbf{b}$ is the density of the resultant

[iv] This lemma gives, in our case, the linear dependence of the traction force on the surface normal, namely:

$$\mathbf{t}(t,\mathbf{x},\mathbf{n}(\mathbf{x}))=\mathbb{T}(t,\mathbf{x})\mathbf{n}(\mathbf{x}),$$

where $\mathbb{T}$ is the flux of the traction force, called the Cauchy stress tensor. Indeed, this statement holds under additional assumption that the traction force does not depend on other differential geometric properties of the surface, e.g. Gaussian curvature. For more details see [Hutter and Jöhnk, 2010], subsec. 2.1.2.

of the body (or volume) forces. Combining (1.7) with (1.8) and using again the additivity principle, we obtain the *equations of motion* with appropriate interface conditions:

$$\frac{\partial(\rho\mathbf{v})}{\partial t} + \operatorname{div}(\rho\mathbf{v}\otimes\mathbf{v}) \overset{(1.5)}{=} \rho\frac{\mathrm{D}\mathbf{v}}{\mathrm{D}t} = \operatorname{div}\mathbb{T} + \rho\mathbf{b} \quad \text{in } \omega(t)\setminus\sigma(t), \tag{1.9}$$

$$[\![\rho\mathbf{v}\otimes(\mathbf{v}-\mathbf{w}) - \mathbb{T}]\!]\mathbf{n}_\sigma = \mathbf{0} \quad \text{on } \sigma(t). \tag{1.10}$$

Balance of angular momentum and symmetry of the Cauchy stress tensor

Mathematical expression of the *Balance Law of Angular Momentum* states:

$$\frac{\mathrm{D}}{\mathrm{D}t}\int_{\omega(t)} \mathbf{x}\times\rho\mathbf{v}\,\mathrm{d}v = \oint_{\partial\omega(t)} \mathbf{x}\times\mathbf{t}(\mathbf{n})\,\mathrm{d}a + \int_{\omega(t)} \mathbf{x}\times\rho\mathbf{b}\,\mathrm{d}v. \tag{1.11}$$

Using the following identity[v]:

$$\mathbf{u}\times(\mathbb{A}\mathbf{v}) = (\mathbf{u}\times\mathbb{A})\,\mathbf{v}, \tag{1.12}$$

we can modify the balance law of angular momentum (1.11):

$$\begin{aligned}\frac{\mathrm{D}}{\mathrm{D}t}\int_{\omega(t)} \mathbf{x}\times\rho\mathbf{v}\,\mathrm{d}v &= \oint_{\partial\omega(t)} \mathbf{x}\times(\mathbb{T}\mathbf{n})\,\mathrm{d}a + \int_{\omega(t)} \mathbf{x}\times\rho\mathbf{b}\,\mathrm{d}v = \\ &\overset{(1.12)}{=} \oint_{\partial\omega(t)} (\mathbf{x}\times\mathbb{T})\mathbf{n}\,\mathrm{d}a + \int_{\omega(t)} \mathbf{x}\times\rho\mathbf{b}\,\mathrm{d}v = \\ &\overset{(1.1)}{=} \int_{\omega(t)\setminus\sigma(t)} \operatorname{div}(\mathbf{x}\times\mathbb{T}) + \mathbf{x}\times\rho\mathbf{b}\,\mathrm{d}v + \int_{\sigma(t)} [\![\mathbf{x}\times\mathbb{T}]\!]\mathbf{n}_\sigma\,\mathrm{d}a. \end{aligned} \tag{1.13}$$

Let us recast the first term in the volume integral into a more convenient form:

$$\begin{aligned}\operatorname{div}(\mathbf{x}\times\mathbb{T}) &= \frac{\partial}{\partial x_j}[\mathbf{x}\times\mathbb{T}]_{ij}\,\mathbf{e}_i = \frac{\partial}{\partial x_j}(\varepsilon_{ikl}x_k\tau_{lj})\,\mathbf{e}_i = \\ &= \varepsilon_{ikl}\frac{\partial x_k}{\partial x_j}\tau_{lj}\mathbf{e}_i + \varepsilon_{ikl}x_k\frac{\partial\tau_{lj}}{\partial x_j}\mathbf{e}_i = \\ &= \mathbb{I}\,\dot{\times}\,\mathbb{T} + \mathbf{x}\times(\operatorname{div}\mathbb{T}), \end{aligned} \tag{1.14}$$

where the dot-cross product $\dot{\times}$ is defined:

$$\mathbb{A}\,\dot{\times}\,\mathbb{B} \coloneqq \varepsilon_{ijk}A_{jl}B_{kl}\mathbf{e}_i,$$

and $\mathbb{I}$ denotes the identity tensor.

[v] Cartesian coordinates of the cross product $\mathbf{u}\times\mathbb{A}$ are given by the following procedure:

$$\begin{aligned}\mathbf{u}\times\mathbb{A} &= u_k\mathbf{e}_k\times A_{lj}\mathbf{e}_l\otimes\mathbf{e}_j = u_kA_{lj}(\mathbf{e}_k\times\mathbf{e}_l)\otimes\mathbf{e}_j = u_kA_{lj}(\varepsilon_{ikl}\mathbf{e}_i)\otimes\mathbf{e}_j = \\ &= \varepsilon_{ikl}u_kA_{lj}\mathbf{e}_i\otimes\mathbf{e}_j = [\mathbf{u}\times\mathbb{A}]_{ij}\,\mathbf{e}_i\otimes\mathbf{e}_j.\end{aligned}$$

Using the generalised Reynolds' theorem (1.2), we can transform the right-hand side into:

$$\begin{aligned}\frac{\mathrm{D}}{\mathrm{D}t}\int_{\omega(t)}\mathbf{x}\times\rho\mathbf{v}\,\mathrm{d}v &= \int_{\omega(t)\setminus\sigma(t)}\frac{\mathrm{D}}{\mathrm{D}t}(\rho\mathbf{x}\times\mathbf{v})+(\rho\mathbf{x}\times\mathbf{v})\,\mathrm{div}\,\mathbf{v}\,\mathrm{d}v+\\ &\qquad+\int_{\sigma(t)}[\![\rho\,(\mathbf{x}\times\mathbf{v})\otimes(\mathbf{v}-\mathbf{w})]\!]\mathbf{n}_\sigma\,\mathrm{d}a=\\ &=\int_{\omega(t)\setminus\sigma(t)}(\mathbf{x}\times\mathbf{v})\left(\frac{\mathrm{D}\rho}{\mathrm{D}t}+\rho\,\mathrm{div}\,\mathbf{v}\right)+\rho\frac{\mathrm{D}\mathbf{x}}{\mathrm{D}t}\times\mathbf{v}+\rho\mathbf{x}\times\frac{\mathrm{D}\mathbf{v}}{\mathrm{D}t}\,\mathrm{d}v+\\ &\qquad+\int_{\sigma(t)}[\![\rho\,(\mathbf{x}\times\mathbf{v})\otimes(\mathbf{v}-\mathbf{w})]\!]\mathbf{n}_\sigma\,\mathrm{d}a=\\ &\overset{(1.5)}{=}\int_{\omega(t)\setminus\sigma(t)}\mathbf{x}\times\rho\frac{\mathrm{D}\mathbf{v}}{\mathrm{D}t}\,\mathrm{d}v+\int_{\sigma(t)}[\![\rho\,(\mathbf{x}\times\mathbf{v})\otimes(\mathbf{v}-\mathbf{w})]\!]\mathbf{n}_\sigma\,\mathrm{d}a,\end{aligned}\tag{1.15}$$

where we used the fact that $\mathrm{D}\mathbf{x}/\mathrm{D}t\times\mathbf{v}=\mathbf{v}\times\mathbf{v}=\mathbf{0}$. Finally, putting together (1.13) with (1.15) and using both (1.14) and the balance of linear momentum (1.9) we assert:

$$\int_{\omega(t)}\mathbb{I}\dot{\times}\mathbb{T}\,\mathrm{d}v+\int_{\sigma(t)}[\![\mathbf{x}\times(\rho\,(\mathbf{v}-\mathbf{w})\otimes\mathbf{v}-\mathbb{T})]\!]\mathbf{n}_\sigma\,\mathrm{d}a=\mathbf{0},$$

which implies:

$$\mathbb{I}\dot{\times}\mathbb{T}=\varepsilon_{ijk}\tau_{kj}\mathbf{e}_i=\mathbf{0}\to\mathbb{T}=\mathbb{T}^T\quad\text{in }\omega(t)\setminus\sigma(t),\tag{1.16}$$

$$[\![\mathbf{x}\times(\rho\,(\mathbf{v}-\mathbf{w})\otimes\mathbf{v}-\mathbb{T})]\!]\mathbf{n}_\sigma=\mathbf{0}\quad\text{on }\sigma(t).\tag{1.17}$$

Obviously, interface jump pertaining to the motion equations (1.10) already yield (1.17). Thus, angular momentum jump conditions are redundant.

Conservation of energy and energy equation

The *Conservation of Energy* states that the time rate of change of total energy—consisting of kinetic and internal parts—equals the rate of work of the surface and body forces along with the other sources of energy. We assume that the energy trasfer is of purely thermo-mechanical origin. The Conservation of Energy can be expressed mathematically as follows:

$$\frac{\mathrm{D}}{\mathrm{D}t}\int_{\omega(t)}\rho e+\frac{1}{2}\rho|\mathbf{v}|^2\,\mathrm{d}v=\oint_{\partial\omega(t)}(\mathbb{T}\mathbf{n})\cdot\mathbf{v}-\mathbf{q}\cdot\mathbf{n}\,\mathrm{d}a+\int_{\omega(t)}\rho\mathbf{b}\cdot\mathbf{v}+\rho b_e\,\mathrm{d}v,\tag{1.18}$$

where e is the internal energy density, $\mathbf{q}$ is the heat flux through boundary and b_e is the heat supply density.

The first term on the right-hand side can be rewritten as follows:

$$\begin{aligned}\oint_{\partial\omega(t)}(\mathbb{T}\mathbf{n})\cdot\mathbf{v}-\mathbf{q}\cdot\mathbf{n}\,\mathrm{d}a&=\oint_{\partial\omega(t)}(\mathbb{T}^T\mathbf{v})\cdot\mathbf{n}-\mathbf{q}\cdot\mathbf{n}\,\mathrm{d}a=\\ &\overset{(1.1)}{=}\int_{\omega(t)\setminus\sigma(t)}\mathrm{div}\,(\mathbb{T}^T\mathbf{v}-\mathbf{q})\,\mathrm{d}v+\int_{\sigma(t)}[\![\mathbb{T}^T\mathbf{v}-\mathbf{q}]\!]\cdot\mathbf{n}_\sigma\,\mathrm{d}a=\\ &=\int_{\omega(t)\setminus\sigma(t)}\mathrm{div}\,\mathbb{T}\cdot\mathbf{v}+\mathbb{T}:\nabla\mathbf{v}-\mathrm{div}\,\mathbf{q}\,\mathrm{d}v+\\ &\qquad+\int_{\sigma(t)}[\![\mathbb{T}^T\mathbf{v}-\mathbf{q}]\!]\cdot\mathbf{n}_\sigma\,\mathrm{d}a,\end{aligned}\tag{1.19}$$

where : means the dot product of tensors (for definition, see Appendix A: Notation). Since we already know that Cauchy stress tensor is symmetric, we can write $\mathbb{T} : \nabla \mathbf{v} = \mathbb{T} : \mathbb{D}$, where $\mathbb{D}$ is the symmetric part of the velocity gradient, i.e. $\mathbb{D} := 1/2(\nabla \mathbf{v} + (\nabla \mathbf{v})^T)$.

The left-hand side of (1.18) can be again—with aid of the Reynolds' theorem (1.2) for $f = \rho E = \rho(e + 1/2|\mathbf{v}|^2)$—transformed into:

$$\begin{aligned}
\frac{\mathrm{D}}{\mathrm{D}t}\int_{\omega(t)} \rho e + \frac{1}{2}\rho|\mathbf{v}|^2 \,\mathrm{d}v = \int_{\omega(t)\setminus\sigma(t)} \frac{\mathrm{D}}{\mathrm{D}t}\left(\rho e + \frac{1}{2}\rho|\mathbf{v}|^2\right) + \left(\rho e + \frac{1}{2}\rho|\mathbf{v}|^2\right) \operatorname{div}\mathbf{v} \,\mathrm{d}v + \\
+ \int_{\sigma(t)} [\![\left(\rho e + \frac{1}{2}\rho|\mathbf{v}|^2\right)(\mathbf{v} - \mathbf{w})]\!] \cdot \mathbf{n}_\sigma \,\mathrm{d}a = \\
= \int_{\omega(t)\setminus\sigma(t)} \left(e + \frac{1}{2}|\mathbf{v}|^2\right)\left(\frac{\mathrm{D}\rho}{\mathrm{D}t} + \rho \operatorname{div}\mathbf{v}\right) + \rho\frac{\mathrm{D}e}{\mathrm{D}t} + \rho\frac{\mathrm{D}\mathbf{v}}{\mathrm{D}t}\cdot\mathbf{v}\mathrm{d}v + \\
+ \int_{\sigma(t)} [\![\left(\rho e + \frac{1}{2}\rho|\mathbf{v}|^2\right)(\mathbf{v} - \mathbf{w})]\!] \cdot \mathbf{n}_\sigma \,\mathrm{d}a = \\
\overset{(1.5)}{=} \int_{\omega(t)\setminus\sigma(t)} \left[\rho\frac{\mathrm{D}e}{\mathrm{D}t} + \rho\frac{\mathrm{D}\mathbf{v}}{\mathrm{D}t}\cdot\mathbf{v}\right] \mathrm{d}v + \\
+ \int_{\sigma(t)} [\![\left(\rho e + \frac{1}{2}\rho|\mathbf{v}|^2\right)(\mathbf{v} - \mathbf{w})]\!] \cdot \mathbf{n}_\sigma \,\mathrm{d}a.
\end{aligned} \tag{1.20}$$

For the reduced local form of the energy conservation law (balance of internal energy), we need to use the balance of linear momentum (1.9), symmetry of the stress tensor (1.16) (plus the consequence that $\mathbb{T} : \nabla \mathbf{v} = \mathbb{T} : \mathbb{D}$), the modified right hand side (1.19) and again the additivity principle:

$$\rho\frac{\mathrm{D}e}{\mathrm{D}t} = \mathbb{T} : \mathbb{D} - \operatorname{div}\mathbf{q} + \rho b_e \qquad \text{in } \omega(t) \setminus \sigma(t), \tag{1.21}$$

$$0 = [\![\left(\rho e + \frac{1}{2}\rho|\mathbf{v}|^2\right)(\mathbf{v} - \mathbf{w}) - \mathbb{T}\mathbf{v} + \mathbf{q}]\!] \cdot \mathbf{n}_\sigma \quad \text{on } \sigma(t). \tag{1.22}$$

Entropy production and entropy inequality

The *Second Law of Thermodynamics* states that the total entropy production, i.e. the total change of entropy minus the contribution due to the entropy flux and entropy sources, is always non-negative, which is expressed mathematically:

$$\frac{\mathrm{D}}{\mathrm{D}t}\int_{\omega(t)} \rho\eta \,\mathrm{d}v - \int_{\omega(t)} \rho b_\eta \,\mathrm{d}v + \oint_{\partial\omega(t)} \mathbf{q}_\eta \cdot \mathbf{n} \,\mathrm{d}a \geq 0, \tag{1.23}$$

where η is the entropy density, b_η is the entropy source and $\mathbf{q}_\eta$ is the entropy flux through the boundary.

Applying the Reynolds Transport Theorem (1.2) to the first term of the balance (1.23) and using the continuity equation (1.5), we will get the local form of the entropy inequality with the appropriate interface jump condition:

$$\rho\frac{\mathrm{D}\eta}{\mathrm{D}t} - \rho b_\eta + \operatorname{div}\mathbf{q}_\eta \geq 0 \quad \text{in } \omega(t) \setminus \sigma(t), \tag{1.24}$$

$$[\![\rho\eta(\mathbf{v} - \mathbf{w}) + \mathbf{q}_\eta]\!] \cdot \mathbf{n}_\sigma \geq 0 \quad \text{on } \sigma(t). \tag{1.25}$$

1.3 Enthalpy method

In this section we present the thermodynamical potential suitable to our problem. Using the definition of the enthalpy, we derive the temperature equation that expresses mathematically the local form of the energy conservation law.

1.3.1 Temperature equation

We start out from the fundamental equation of the internal energy density in the form:

$$e = e\left(\eta, \frac{1}{\rho}\right), \tag{1.26}$$

where we assume that e is a function of the class C^2, which is strictly convex in both variables. The reasons for such requirements will be unveiled in the following.

Because of the smoothness of the function e, the following definitions have sense:

$$p^{\text{th}} \coloneqq -\left(\frac{\partial e}{\partial(1/\rho)}\right)_{\eta}, \quad \theta \coloneqq \left(\frac{\partial e}{\partial \eta}\right)_{1/\rho}, \tag{1.27}$$

where p^{th} is the thermodynamic pressure and θ is the thermodynamic temperature. Since we assumed that e is twice continuously differentiable and strictly convex, we see that $\partial^2 e/\partial(1/\rho)^2 > 0$. Due to the *Inverse Function Theorem* (see e.g. [Evans, 1998], Appendix C.5), there exists a C^1 function, which we will for simplicity denote $1/\rho$, such that:

$$\frac{1}{\rho} = \frac{1}{\rho}(\eta, p^{\text{th}}).$$

Now we can rewrite the internal energy density in terms of η and p^{th}:

$$e = \tilde{e}(\eta, p^{\text{th}}) \coloneqq e\left(\eta, \frac{1}{\rho}(\eta, p^{\text{th}})\right). \tag{1.28}$$

We are now ready to define our preferred thermodynamic potential as the Legendre transform of the internal energy e with respect to $1/\rho$, i.e. enthalpy:

$$h(\eta, p^{\text{th}}) \coloneqq \tilde{e}(\eta, p^{\text{th}}) + p^{\text{th}} \frac{1}{\rho}(\eta, p^{\text{th}}). \tag{1.29}$$

Natural variables of the enthalpy are the entropy η and the pressure p^{th}, which is not convenient, since we are unable to measure entropy directly. It is therefore preferable to exchange the entropy for the thermodynamic temperature θ[vi]. As a

[vi] The pressure and temperature are natural variables of a different thermodynamic potential, namely the *Gibbs potential* G, which we could have used directly, but thus we would loose the physical interpretation of the jump across the singular surface—see section Enthalpy interface condition.

consequence of our definition of enthalpy (1.29) we get:

$$\left(\frac{\partial h}{\partial \eta}\right)_{p^{\mathrm{th}}} = \left(\frac{\partial e}{\partial \eta}\right)_{1/\rho} + \left(\frac{\partial e}{\partial (1/\rho)}\right)_{\eta} \left(\frac{\partial (1/\rho)}{\partial \eta}\right)_{p^{\mathrm{th}}} + p^{\mathrm{th}} \left(\frac{\partial (1/\rho)}{\partial \eta}\right)_{p^{\mathrm{th}}} \overset{(1.27)}{=} \theta, \quad (1.30)$$

$$\left(\frac{\partial h}{\partial p^{\mathrm{th}}}\right)_{\eta} = \left(\frac{\partial e}{\partial (1/\rho)}\right)_{\eta} \left(\frac{\partial (1/\rho)}{\partial p^{\mathrm{th}}}\right)_{\eta} + \frac{1}{\rho}(\eta, p^{\mathrm{th}}) + p^{\mathrm{th}} \left(\frac{\partial (1/\rho)}{\partial p^{\mathrm{th}}}\right)_{\eta} \overset{(1.27)}{=} \frac{1}{\rho}. \quad (1.31)$$

If we knew that $\partial^2 h/\partial \eta^2 > 0$, we could express this time entropy η in terms of thermodynamic temperature and pressure to get the suitable potential. It is required to show that enthalpy is a strictly convex function with respect to entropy. Nevertheless we know that the internal energy e is a strictly convex function in both its variables, which gives (using Sylvester's criterion on a Hessian matrix of the smooth function e):

$$\frac{\partial^2 e}{\partial \eta^2} > 0, \ \frac{\partial^2 e}{\partial (1/\rho)^2} > 0, \ \frac{\partial^2 e}{\partial \eta^2} \frac{\partial^2 e}{\partial (1/\rho)^2} > \left(\frac{\partial^2 e}{\partial \eta \partial (1/\rho)}\right)^2. \quad (1.32)$$

The differentiation of the thermodynamic pressure (1.27) with respect to entropy η yields:

$$0 = -\frac{\partial^2 e}{\partial \eta \partial (1/\rho)} - \frac{\partial^2 e}{\partial (1/\rho)^2} \frac{\partial (1/\rho)}{\partial \eta}. \quad (1.33)$$

Finally, we can express the second derivative of enthalpy in the following way:

$$\begin{aligned} \frac{\partial^2 h}{\partial \eta^2} &\overset{(1.30)}{=} \frac{\partial \theta}{\partial \eta} \overset{(1.27)}{=} \frac{\partial^2 e}{\partial \eta^2} + \frac{\partial^2 e}{\partial \eta \partial (1/\rho)} \frac{\partial (1/\rho)}{\partial \eta} = \\ &\overset{(1.33)}{=} \frac{\partial^2 e}{\partial \eta^2} - \left(\frac{\partial^2 e}{\partial \eta \partial (1/\rho)}\right)^2 \left(\frac{\partial^2 e}{\partial (1/\rho)^2}\right)^{-1} \overset{(1.32)}{>} 0. \end{aligned}$$

Just as a remark, it is possible to show that enthalpy h is strictly concave in pressure p^{th} (proof is similar, see lecture notes [Evans, 2018]).

In view of the Inverse Function Theorem we are now allowed to define the enthalpy h as a function of the temperature θ and the pressure p^{th}:

$$\tilde{h}(\theta, p^{\mathrm{th}}) := h\left(\eta(\theta, p^{\mathrm{th}}), p^{\mathrm{th}}\right). \quad (1.34)$$

To simplify the notation, we will denote this new function by the same symbol h. Next we need to give sense to the material derivative of the enthalpy potential:

$$\frac{\mathrm{D}h}{\mathrm{D}t} = \left(\frac{\partial h}{\partial \theta}\right)_{p^{\mathrm{th}}} \frac{\mathrm{D}\theta}{\mathrm{D}t} + \left(\frac{\partial h}{\partial p^{\mathrm{th}}}\right)_{\theta} \frac{\mathrm{D}p^{\mathrm{th}}}{\mathrm{D}t}, \quad (1.35)$$

$$\left(\frac{\partial h}{\partial \theta}\right)_{p^{\mathrm{th}}} \overset{(1.34)}{=} \left(\frac{\partial h}{\partial \eta}\right)_{p^{\mathrm{th}}} \left(\frac{\partial \eta}{\partial \theta}\right)_{p^{\mathrm{th}}} \overset{(1.27)}{=} \theta \left(\frac{\partial \eta}{\partial \theta}\right)_{p^{\mathrm{th}}} =: c_p, \quad (1.36)$$

$$\left(\frac{\partial h}{\partial p^{\mathrm{th}}}\right)_{\theta} \overset{(1.34)}{=} \left(\frac{\partial h}{\partial \eta}\right)_{\theta} \left(\frac{\partial \eta}{\partial p^{\mathrm{th}}}\right)_{\theta} + \left(\frac{\partial h}{\partial p^{\mathrm{th}}}\right)_{\theta} \overset{(1.27)}{=} \theta \left(\frac{\partial \eta}{\partial p^{\mathrm{th}}}\right)_{\theta} + \frac{1}{\rho}. \quad (1.37)$$

In (1.36) we defined the molar heat capacity at constant pressure c_p. It only remains to express $\partial \eta/\partial p^{\mathrm{th}}$ by means of measurable quantities. To this end we

will use both the second and the first law of thermodynamics:

$$\theta \mathrm{d}\eta = \theta \left(\frac{\partial \eta}{\partial \theta}\right)_{p^{\mathrm{th}}} \mathrm{d}\theta + \theta \left(\frac{\partial \eta}{\partial p^{\mathrm{th}}}\right)_{\theta} \mathrm{d}p^{\mathrm{th}} \overset{(1.36)}{=} c_p \mathrm{d}\theta + \theta \left(\frac{\partial \eta}{\partial p^{\mathrm{th}}}\right)_{\theta} \mathrm{d}p^{\mathrm{th}} \tag{1.38}$$

$$\begin{aligned}\theta \mathrm{d}\eta = \mathrm{d}e + p^{\mathrm{th}} \mathrm{d}\frac{1}{\rho} &= \left(\frac{\partial e}{\partial \theta}\right)_{p^{\mathrm{th}}} \mathrm{d}\theta + \left(\frac{\partial e}{\partial p^{\mathrm{th}}}\right)_{\theta} \mathrm{d}p^{\mathrm{th}} + \\ &+ p^{\mathrm{th}} \left(\frac{\partial (1/\rho)}{\partial \theta}\right)_{p^{\mathrm{th}}} \mathrm{d}\theta + p^{\mathrm{th}} \left(\frac{\partial (1/\rho)}{\partial p^{\mathrm{th}}}\right)_{\theta} \mathrm{d}p^{\mathrm{th}} = \\ = \left[\left(\frac{\partial e}{\partial \theta}\right)_{p^{\mathrm{th}}} + p^{\mathrm{th}} \left(\frac{\partial (1/\rho)}{\partial \theta}\right)_{p^{\mathrm{th}}}\right] \mathrm{d}\theta &+ \left[\left(\frac{\partial e}{\partial p^{\mathrm{th}}}\right)_{\theta} + p^{\mathrm{th}} \left(\frac{\partial (1/\rho)}{\partial p^{\mathrm{th}}}\right)_{\theta}\right] \mathrm{d}p^{\mathrm{th}}. \end{aligned} \tag{1.39}$$

If we use the symmetry of the second mixed derivatives of η (often called as *Maxwell relations*), then (1.38) yields:

$$\frac{\partial c_p}{\partial p^{\mathrm{th}}} = \theta \frac{\partial^2 \eta}{\partial p^{\mathrm{th}} \partial \theta} = \theta \frac{\partial^2 \eta}{\partial \theta \partial p^{\mathrm{th}}} = \frac{\partial}{\partial \theta} \left(\theta \left(\frac{\partial \eta}{\partial p^{\mathrm{th}}}\right)_{\theta}\right) - \left(\frac{\partial \eta}{\partial p^{\mathrm{th}}}\right)_{\theta}. \tag{1.40}$$

Following the same steps, we can get from (1.39)

$$\begin{aligned}\frac{\partial c_p}{\partial p^{\mathrm{th}}} &= \frac{\partial^2 e}{\partial p^{\mathrm{th}} \partial \theta} + \left(\frac{\partial (1/\rho)}{\partial \theta}\right)_{p^{\mathrm{th}}} + p^{\mathrm{th}} \frac{\partial^2 (1/\rho)}{\partial p^{\mathrm{th}} \partial \theta} = \\ &= \frac{\partial^2 e}{\partial \theta \partial p^{\mathrm{th}}} + p^{\mathrm{th}} \frac{\partial^2 (1/\rho)}{\partial \theta \partial p^{\mathrm{th}}} + \left(\frac{\partial (1/\rho)}{\partial \theta}\right)_{p^{\mathrm{th}}} = \\ &= \frac{\partial}{\partial \theta} \left[\left(\frac{\partial e}{\partial p^{\mathrm{th}}}\right)_{\theta} + p^{\mathrm{th}} \left(\frac{\partial (1/\rho)}{\partial p^{\mathrm{th}}}\right)_{\theta}\right] + \left(\frac{\partial (1/\rho)}{\partial \theta}\right)_{p^{\mathrm{th}}} = \\ &\overset{(1.39)}{=} \frac{\partial}{\partial \theta} \left(\theta \left(\frac{\partial \eta}{\partial p^{\mathrm{th}}}\right)_{\theta}\right) + \left(\frac{\partial (1/\rho)}{\partial \theta}\right)_{p^{\mathrm{th}}}. \end{aligned} \tag{1.41}$$

If we compare (1.40) with (1.41), we obtain the desired expression:

$$\left(\frac{\partial \eta}{\partial p^{\mathrm{th}}}\right)_{\theta} = -\left(\frac{\partial (1/\rho)}{\partial \theta}\right)_{p^{\mathrm{th}}} = -\left(\frac{\partial V}{\partial \theta}\right)_{p^{\mathrm{th}}} = -\frac{\beta_{\mathrm{V}}}{\rho}. \tag{1.42}$$

In the last expression we used the thermal expansion coefficient β_{V}, which reads:

$$\beta_{\mathrm{V}} \coloneqq \frac{1}{V} \left(\frac{\partial V}{\partial \theta}\right)_{p^{\mathrm{th}}}.$$

Finally, if we plug (1.42) into (1.37), combine this with (1.36) and substitute both into equation (1.35), we obtain the final form of the material time derivative of enthalpy expressed in thermodynamical temperature and pressure:

$$\frac{\mathrm{D}h}{\mathrm{D}t} = c_p \frac{\mathrm{D}\theta}{\mathrm{D}t} + \frac{1}{\rho}(1 - \beta_{\mathrm{V}}\theta) \frac{\mathrm{D}p^{\mathrm{th}}}{\mathrm{D}t}. \tag{1.43}$$

On the other hand we can use the definition of enthalpy and express its balance:

$$\begin{aligned}\rho \frac{\mathrm{D}h}{\mathrm{D}t} &\overset{(1.29)}{=} \rho \frac{\mathrm{D}e}{\mathrm{D}t} + \frac{\mathrm{D}p^{\mathrm{th}}}{\mathrm{D}t} - \frac{p^{\mathrm{th}}}{\rho} \frac{\mathrm{D}\rho}{\mathrm{D}t} = \\ &\overset{(1.21),(1.5)}{=} \mathbb{T} : \mathbb{D} - \operatorname{div} \mathbf{q} + \rho b_e + \frac{\mathrm{D}p^{\mathrm{th}}}{\mathrm{D}t} + p^{\mathrm{th}} \operatorname{div} \mathbf{v}. \end{aligned} \tag{1.44}$$

To obtain the temperature equation, it remains to combine the last two results (1.43) and (1.44):

$$\rho c_p \frac{\mathrm{D}\theta}{\mathrm{D}t} = \mathbb{T}^\delta : \mathbb{D}^\delta - \operatorname{div} \mathbf{q} + \rho b_e + (m + p^{\mathrm{th}}) \operatorname{div} \mathbf{v} + \beta_{\mathrm{V}} \theta \frac{\mathrm{D}p^{\mathrm{th}}}{\mathrm{D}t}, \tag{1.45}$$

where $m := 1/3 \operatorname{Tr} \mathbb{T}$ is the mean normal stress and $\mathbb{A}^\delta := \mathbb{A} - 1/3(\operatorname{Tr} \mathbb{A})\mathbb{I}$ is the deviatoric part of the tensor $\mathbb{A}$. The equation (1.45) represents the time evolution of the thermodynamic temperature.

1.3.2 Enthalpy interface condition

Since we transformed the local internal energy balance, we need to express the jump quantity accordingly. Let us start from the energy interface condition (1.22), since we know that $[\![\rho(\mathbf{v} - \mathbf{w})]\!] \cdot \mathbf{n}_\sigma = 0$, we can define $\mathcal{M} := \rho^+ (\mathbf{v}^+ - \mathbf{w}) \cdot \mathbf{n}_\sigma = \rho^- (\mathbf{v}^- - \mathbf{w}) \cdot \mathbf{n}_\sigma$. Now if we decompose the Cauchy stress tensor isolating its viscous part, i.e.: $\mathbb{T} = -p^{\mathrm{th}}\mathbb{I} + \mathbb{S}$ (such decomposition is only natural for compressible Navier-Stokes equations), we can modify (1.22):

$$[\![\rho E(\mathbf{v}-\mathbf{w}) - \mathbb{T}\mathbf{v} + \mathbf{q}]\!] \cdot \mathbf{n}_\sigma = \mathcal{M}[\![E]\!] - [\![\left(-p^{\mathrm{th}}\mathbb{I} + \mathbb{S}\right)\mathbf{v}]\!] \cdot \mathbf{n}_\sigma + [\![\mathbf{q}]\!] \cdot \mathbf{n}_\sigma = 0. \tag{1.46}$$

If we assume that no jump in pressure occurs across the singular surface (which holds if we exclude phenomena like shock waves and neglect the possible curvature effect of surface tension), mathematically: $[\![p^{\mathrm{th}}]\!] = 0$, then we can modify the second term in (1.46):

$$\begin{aligned} [\![\left(-p^{\mathrm{th}}\mathbb{I} + \mathbb{S}\right)\mathbf{v}]\!] \cdot \mathbf{n}_\sigma &\overset{(1.3)}{=} -[\![p^{\mathrm{th}}(\mathbf{v} - \mathbf{w})]\!] \cdot \mathbf{n}_\sigma + [\![\mathbb{S}\mathbf{v}]\!] \cdot \mathbf{n}_\sigma = \\ &\overset{(1.16)}{=} -\mathcal{M}\left[\!\left[\frac{p^{\mathrm{th}}}{\rho}\right]\!\right] + [\![\mathbb{S}\mathbf{n}_\sigma \cdot \mathbf{v}]\!]. \end{aligned} \tag{1.47}$$

The second term on the right-hand side has now meaning of a power of the friction forces. Additionally if we consider the definition of enthalpy (1.29) we can further express the energy interface condition (1.46) in the form of enthalpy:

$$\mathcal{M}\left[\!\left[e + \frac{p^{\mathrm{th}}}{\rho}\right]\!\right] = \mathcal{M}[\![h]\!] = [\![\mathbb{S}\mathbf{n}_\sigma \cdot \mathbf{v}]\!] - [\![\mathbf{q}]\!] \cdot \mathbf{n}_\sigma - \mathcal{M}\left[\!\left[\frac{1}{2}|\mathbf{v}|^2\right]\!\right]. \tag{1.48}$$

It is customary to denote $\mathrm{L} := [\![h]\!]$, where L has the meaning of latent heat of fusion, in particular $\mathrm{L_m}$ means the latent heat of melting, which will be considered in the rest of the thesis.

To obtain the classical *Stefan condition* we need to neglect all the terms on the right-hand side except for the heat flux jump condition:

$$\mathcal{M}\mathrm{L_m} = -[\![\mathbf{q}]\!] \cdot \mathbf{n}_\sigma. \tag{1.49}$$

The jump condition (1.49) says that the amount of heat, that is given by the difference of heat that enters the melting front from the liquid phase and heat that is sucked away by the solid phase per one second, is consumed solely by the solid-to-liquid phase change of one cubic meter of material of density $\mathcal{M}$.

1.3.3 Mollified parameters

So far we have been describing our domain of interest as two independent continua ω_{l} and ω_{s} separated by the smooth singular surface $\sigma(t)$. It is time to switch our viewpoint and apply the so-called *diffused interface method*, where we consider the domain to be filled with a single fluid with continuously variable material properties. That way there will be only one set of governing equations with interfacial terms accounted for by the addition of the appropriate interface sources. We will demonstrate the procedure on on the example of the enthalpy potential. We will consider heat capacities c_p^{s} and c_p^{l} to be independent of the thermodynamic temperature θ. In view of the temperature derivative of enthalpy (1.36) and the fact that $[\![h]\!] = \mathrm{L_m}$ on $\sigma(t)$, we see that:

$$h(\theta, p^{\mathrm{th}}) = c_p^{\mathrm{s}}(p^{\mathrm{th}})\theta\chi_{(0,\theta_{\mathrm{m}})}(\theta) + \left(\mathrm{L_m}(p^{\mathrm{th}}) + c_p^{\mathrm{l}}(p^{\mathrm{th}})\theta\right)\chi_{[\theta_{\mathrm{m}},\infty)}(\theta) + h_0(p^{\mathrm{th}}), \quad (1.50)$$

where $\chi_{(\theta_a,\theta_b)}(\theta)$ is the characteristic function of the interval (θ_a, θ_b) and h_0 is an enthalpy of formation, which is a tabulated quantity. In the following, the pressure dependence of material coefficients in (1.50) will be unimportant. We restrict ourselves to a simplified formula:

$$h(\theta) = c_p^{\mathrm{s}}\theta\chi_{(0,\theta_{\mathrm{m}})}(\theta) + \left(\mathrm{L_m} + c_p^{\mathrm{l}}\theta\right)\chi_{[\theta_{\mathrm{m}},\infty)}(\theta) + h_0, \quad (1.51)$$

which can be viewed as the original equation (1.50) at a reference pressure p_0— e.g., atmospheric or ambient pressure.

From the computational point of view, it is impossible to work with distributions. To overcome such obstacle it is necessary to provide regular approximations of such distributions. We will therefore mollify the material parameters and use continuous approximations of Heavyside step function and Dirac delta distribution. Graphic interpretation of regularisation is depicted on Figure 1.3. The sharp interface will be thus spread over a band of width 2ϵ around the melting temperature θ_{m}.

We will provide the relation (1.51) for the product ρh as well. This is reasonable, because the product of two distributions, that will emerge after differentiation of ρ and h, cannot be generally treated as a distribution. Therefore:

$$\rho h(\theta) = \rho^{\mathrm{s}} c_p^{\mathrm{s}}\theta\chi_{(0,\theta_{\mathrm{m}})}(\theta) + \left(\rho^{\mathrm{l}}\mathrm{L_m} + \rho^{\mathrm{l}} c_p^{\mathrm{l}}\theta\right)\chi_{[\theta_{\mathrm{m}},\infty)}(\theta) + h_0^{\rho}. \quad (1.52)$$

Now we can express the temperature equation (1.45) in the conservative form:

$$\frac{\partial \rho h}{\partial t} + \operatorname{div}(\rho h \mathbf{v}) = \rho\frac{\mathrm{D}h}{\mathrm{D}t} \overset{(1.44)}{=} \mathbb{T} : \mathbb{D} - \operatorname{div}\mathbf{q} + \rho b_e + \frac{\mathrm{D}p^{\mathrm{th}}}{\mathrm{D}t} + p^{\mathrm{th}}\operatorname{div}\mathbf{v}.$$

Using the expression (1.52), we can modify the left hand side of the previous formula to get an alternative form of the temperature equation:

$$\frac{\partial \rho h}{\partial \theta}\frac{\partial \theta}{\partial t} + \operatorname{div}(\rho h \mathbf{v}) = \mathbb{T} : \mathbb{D} - \operatorname{div}\mathbf{q} + \rho b_e + \frac{\mathrm{D}p^{\mathrm{th}}}{\mathrm{D}t} + p^{\mathrm{th}}\operatorname{div}\mathbf{v}. \quad (1.53)$$

Presence of such a "mushy" region is also physically meaningful, since phase transitions take place at regions of finite thickness[vii]. As a result of the mollifica-

[vii] The thickness vary from orders of Angstroms to centimeters and depends on many factors. Typically, thicker phase-transition regions result from phenomena of thermodynamical metastability, which will be not considered in the thesis. Those regions tend to have dendritic or columnar microstructure. For details, the reader can refer to [Alexiades and Solomon, 1993].

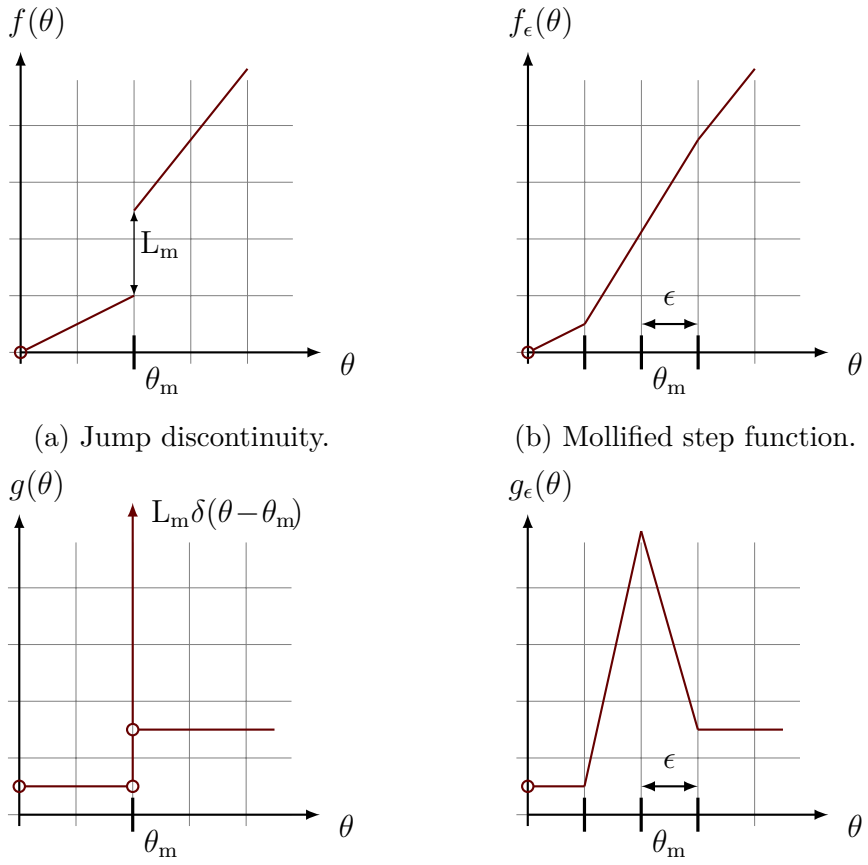

(a) Jump discontinuity.

(b) Mollified step function.

(c) Function with singularity at θ_m.

(d) Continuous approximation of $g(\theta)$.

Figure 1.3: Illustration of piecewise linear continuous approximation of two archetypal distributions, (a) might describe enthalpy given by (1.51), graph of $g(\theta) = \mathrm{d}f(\theta)/\mathrm{d}\theta$ (in the sense of distributions) in figure (c) describes the temperature dependence of the heat capacity c_p.

tion, the evolution of the continuum will be described by a single system of PDEs, containing strongly non-homogeneous (but continuous) material coefficients.

1.4 Résumé

For the sake of clarity we will make a summary of the previous content in the form of two juxtaposed formulations of the problem.

1.4.1 Sharp-interface formulation

Only as a reminder: we consider the domain to be divided by the singular surface σ into two subdomains ω_s and ω_l (as depicted in Figure 1.4) filled with two independent continua governed by their particular systems of governing equations supplemented by the jump conditions as a mean of communication between the two phases. For fully Eulerian mathematical description, see Table 1.1.

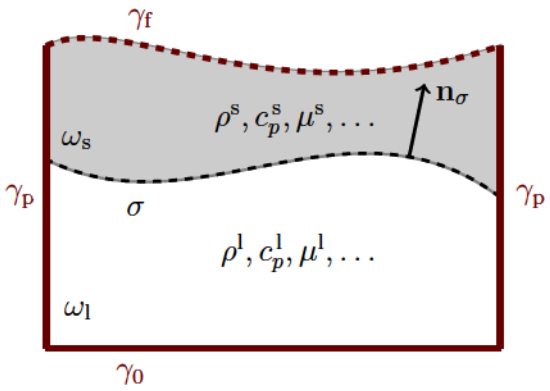

Figure 1.4: Sharp-interface formulation – description of the domain.

	Solid domain ω_s	**Luquid domain** ω_l
Governing equations		
Mass	$\frac{D\rho^s}{Dt} + \rho^s \operatorname{div} \mathbf{v}^s = 0$	$\frac{D\rho^l}{Dt} + \rho^l \operatorname{div} \mathbf{v}^l = 0$
Momentum	$\rho^s \frac{D\mathbf{v}^s}{Dt} = \operatorname{div} \mathbb{T}^s + \rho^s \mathbf{b}^s$	$\rho^l \frac{D\mathbf{v}^l}{Dt} = \operatorname{div} \mathbb{T}^l + \rho^l \mathbf{b}^l$
Ang. mom.	$\mathbb{T}^s = (\mathbb{T}^s)^T$	$\mathbb{T}^l = \left(\mathbb{T}^l\right)^T$
Temperature	$\rho^s c_p^s \frac{D\theta^s}{Dt} = \mathbb{T}^s : \mathbb{D}^s - \operatorname{div} \mathbf{q}^s + \rho^s b_e^s + p^{th,s} \operatorname{div} \mathbf{v}^s + \beta_V^s \theta^s \frac{Dp^{th,s}}{Dt}$	$\rho^l c_p^l \frac{D\theta^l}{Dt} = \mathbb{T}^l : \mathbb{D}^l - \operatorname{div} \mathbf{q}^l + \rho^l b_e^l + p^{th,l} \operatorname{div} \mathbf{v}^l + \beta_V^l \theta^l \frac{Dp^{th,l}}{Dt}$
Jump conditions[a,b]		
Mass	$[\![\rho(\mathbf{v} - \mathbf{w})]\!] \cdot \mathbf{n}_\sigma = 0$	
Momentum	$[\![\rho \mathbf{v} \otimes (\mathbf{v} - \mathbf{w}) - \mathbb{T}]\!] \mathbf{n}_\sigma = \mathbf{0}$	
Enthalpy	$[\![\mathbb{S}\mathbf{n}_\sigma \cdot \mathbf{v}]\!] - [\![\mathbf{q}]\!] \cdot \mathbf{n}_\sigma - \mathcal{M}[\![\frac{1}{2}\lvert\mathbf{v}\rvert^2]\!] = \mathcal{M} L_m$	

Note: [a] Here, jump has the following meaning: $[\![\rho]\!] = \rho^s - \rho^l$.
[b] Jump condtion of angular momentum is omitted due to its redundancy, see sub-subsection of 1.2.2.

Table 1.1: Summary of the sharp-interface formulation.

1.4.2 Diffused-interface formulation

As a diffused-interface problem we denote the formulation with a single domain containing both of the phases, one changing into the other through a band of width 2ϵ (where the metric is given by the temperature), see Figure 1.5.

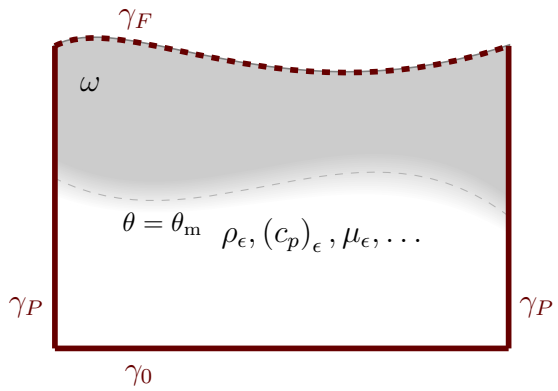

Figure 1.5: Formulation of the diffused-interface problem. The gray dashed line in the middle gives the position of the melting front, where $\theta = \theta_{\mathrm{m}}$.

Evolution of such a problem is governed by the following PDEs:

$$\frac{\mathrm{D}\rho_\epsilon}{\mathrm{D}t} = -\rho_\epsilon \operatorname{div} \mathbf{v}, \tag{1.54}$$

$$\rho_\epsilon \frac{\mathrm{D}\mathbf{v}}{\mathrm{D}t} = \operatorname{div} \mathbb{T}_\epsilon + \rho_\epsilon \mathbf{b}_\epsilon, \tag{1.55}$$

$$\rho_\epsilon \left(c_p\right)_\epsilon \frac{\mathrm{D}\theta}{\mathrm{D}t} = \mathbb{T}_\epsilon : \mathbb{D} - \operatorname{div} \mathbf{q}_\epsilon + \rho_\epsilon \left(b_e\right)_\epsilon + p^{\mathrm{th}} \operatorname{div} \mathbf{v} + \left(\beta_{\mathrm{V}}\right)_\epsilon \theta \frac{\mathrm{D}p^{\mathrm{th}}}{\mathrm{D}t}, \tag{1.56}$$

where we solve for the unknown velocity $\mathbf{v}$, thermodynamic pressure p^{th} and temperature θ. The coefficient approximations are concisely tabulated in Table 1.2.

Material quantity[a]	**Continuous approximation**
$\rho, \mu, k, \beta_{\mathrm{V}}, b_e, \mathbf{q}, \mathbf{b}, \mathbb{T}$	$f_\epsilon = f^{\mathrm{s}} + (f^{\mathrm{l}} - f^{\mathrm{s}}) H^0_\epsilon(\theta - \theta_{\mathrm{m}})$
c_p	$(c_p)_\epsilon = c_p^{\mathrm{s}} + (c_p^{\mathrm{l}} - c_p^{\mathrm{s}}) H^0_\epsilon(\theta - \theta_{\mathrm{m}}) + \mathrm{L}_{\mathrm{m}} \delta^0_\epsilon(\theta - \theta_{\mathrm{m}})$
Special functions	
$H^0_\epsilon(\theta - \theta_{\mathrm{m}})$	$\begin{cases} 0 & \text{if } \theta < \theta_{\mathrm{m}} - \epsilon \\ \frac{\theta - \theta_{\mathrm{m}}}{2\epsilon} - \frac{1}{2} & \text{if } \lvert\theta - \theta_{\mathrm{m}}\rvert \le \epsilon \\ 1 & \text{otherwise} \end{cases}$
$\delta^0_\epsilon(\theta - \theta_{\mathrm{m}})$	$\begin{cases} \frac{1}{\epsilon^2}\left(\epsilon - \frac{(\theta - \theta_{\mathrm{m}})^2}{\lvert\theta - \theta_{\mathrm{m}}\rvert}\right) & \text{if } \lvert\theta - \theta_{\mathrm{m}}\rvert \le \epsilon \\ 0 & \text{otherwise} \end{cases}$

Note: [a] Names of the quantities are given in List of Symbols and Abbreviations.

Table 1.2: Mollified material coefficients.

2. Stefan problem

This chapter deals with the first possible complication that was described in the formulation of the problem presented in the sub-subsection Geometry and boundary conditions. Sole purpose of the folowing chapter is to give an answer (satisfactory, if possible) to a question wheter the tool devised in the section Enthalpy method is powerful enough to track the position of the phase change front. To this end we will benchmark enthalpy method with an analytic solution to the Stefan[i] problem. The analytic solution will be given for all the physically meaningful (and analytically solvable) formulations of the problem.

2.1 Stefan 1D

First, we consider two phase Stefan problem on a semi-infinite one dimensional domain.

2.1.1 Continuous problem

Formulation

Let us consider semi-infinite bar made of homogeneous material with following properties:

- Cross section of the bar is constant along the center line.
- The material is thermally insulated so that no heat escapes through the boudnary of the bar.
- There are no heat sources within the material.

Initially, the material is solid and held at a temperature θ_∞, which is below solidus. At the beginning of the observation heating is applied to the left end of the domain. Position along the center line of the domain is described by an x coordinate, so the end $x = 0$ is heated to a temperature θ_0 which is above the melting temperature of the solid phase denoted as θ_m. Consequently after applying the heat, the material starts to melt and a liquid phase of the material starts to spread from the left end of the bar. We add several assumptions on the two phase problem:

- Both phases are of the same density ρ.
- Thermal properties of the phases—specific heat c_p and conductivity coefficient k—are different but constant within the respective subdomain.
- The only mechanism of heat transfer is conduction—we assume the problem to be static with $\mathbf{v} = \mathbf{0}$.
- Latent heat L_m and melting temperature θ_m are constant.

[i] Josef Stefan (1835–1893) – Austrian physicist, also known for an empiric derivation of the Stefan-Boltzmann law of a blackbody radiation.

- As mentioned earlier, we do not assume metastability or nucleation phenomena to take place.

The interface between the two phases (denoted as σ in the first chapter) reduces in our abstraction to a point whose position at time t is denoted by $s(t)$. Figure 2.1 graphically summarizes the formulation.

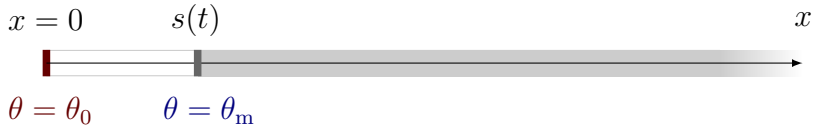

Figure 2.1: Sharp-interface formulation of the one-dimensional Stefan problem on a semi-infinite line. The right end of the bar is heated to a constant temperature θ_0, position of the melting front is denoted $s(t)$.

The temperature distribution within both of the phases of our semi-infinite insulated material is described by the heat equation (1.45), which is significantly reduced since we assume the phase change to be held at a constant pressure. Moreover the material is considered incompressible and stationary ($\mathbf{v} = \mathbf{0}$ in both phases). Finally, if we assume that there are no heat sources and that the heat transfer is governed by the Fourier's law, we obtain the standard heat equation:

$$\rho c_p \frac{\partial \theta}{\partial t} = \operatorname{div}(k \nabla \theta). \tag{2.1}$$

Now, under previous assumptions, we look for both the temeprature distributions $\theta^{\mathrm{l}}(t,x)$, $\theta^{\mathrm{s}}(t,x)$ and the position of the melting front $s(t)$, such that following holds:

Heat equation in liquid region:

$$\frac{\partial \theta^{\mathrm{l}}}{\partial t} = \alpha^{\mathrm{l}} \frac{\partial^2 \theta^{\mathrm{l}}}{\partial x^2}, \qquad 0 < x < s(t), \tag{2.2}$$

Heat equation in solid region:

$$\frac{\partial \theta^{\mathrm{s}}}{\partial t} = \alpha^{\mathrm{s}} \frac{\partial^2 \theta^{\mathrm{s}}}{\partial x^2}, \qquad x \geq s(t). \tag{2.3}$$

Boundary conditions:

$$\begin{aligned} \theta^{\mathrm{l}}(x,t)\Big|_{x=0} &= \theta_0, \\ \lim_{x \to \infty} \theta^{\mathrm{s}}(x,t) &= \theta_\infty, \end{aligned} \tag{2.4}$$

Interface condition:

$$\theta^{\mathrm{l}}(x,t)\Big|_{x=s(t)} = \theta_{\mathrm{m}} = \theta^{\mathrm{s}}(x,t)\Big|_{x=s(t)}, \tag{2.5}$$

Initial condition:

$$\theta^{\mathrm{s}}(x,t)\Big|_{t=0} = \theta_\infty, \tag{2.6}$$

where $\alpha^{\mathrm{l}} = k^{\mathrm{l}}/(\rho c_p^{\mathrm{l}})$ denotes the heat diffusivity coefficient of the liquid phase. Evolution of the melting front position is governed by the classical Stefan condi-

tion (1.49), which in one-dimensional stationary problem takes the form:

$$\rho \mathrm{L_m} w_x = \rho \mathrm{L_m} \frac{\mathrm{d}s}{\mathrm{d}t} = -k^{\mathrm{l}} \frac{\partial \theta^{\mathrm{l}}}{\partial x}\bigg|_{x=s(t)} + k^{\mathrm{s}} \frac{\partial \theta^{\mathrm{s}}}{\partial x}\bigg|_{x=s(t)}. \tag{2.7}$$

Nondimensional variables

We will solve the problem (2.2)-(2.7) analytically using similarity variable. In order to do that it is convenient to formulate the problem nondimensionally—we also demonstrate the procedure of nondimensional formulation on this simple problem, since we will use nondimensional form of the problem quite often. We start with setting the dimensionless temperatures as follows:

$$\widetilde{\theta}^{\mathrm{l}} = \frac{\theta^{\mathrm{l}} - \theta_{\mathrm{m}}}{\theta_0 - \theta_{\mathrm{m}}},$$
$$\widetilde{\theta}^{\mathrm{s}} = \frac{\theta^{\mathrm{s}} - \theta_{\mathrm{m}}}{\theta_{\mathrm{m}} - \theta_\infty}.$$

Substituting furthermore the normalized spatial and temporal coordinates with scales $[x]$ and $[t]$ respectively: $\tilde{x} = x/[x]$, $\tilde{t} = t/[t]$, $\tilde{s} = s/[x]$ into the equation (2.2), we arrive at:

$$\frac{\partial \widetilde{\theta}^{\mathrm{l}}}{\partial \tilde{t}} = \alpha^{\mathrm{l}} \frac{[t]}{[x]^2} \frac{\partial^2 \widetilde{\theta}^{\mathrm{l}}}{\partial \tilde{x}^2},$$

choosing so-called *diffusion time* for the temporal scale $[t] = [x]^2/\alpha^{\mathrm{l}}$ and transforming the boundary and initial conditions (2.4), resp. (2.6), we thus give rise to a nondimensional formulation of the Stefan problem—tildes were dropped for simplicity of notation:

Nondimensional heat equation in liquid region:

$$\frac{\partial \theta^{\mathrm{l}}}{\partial t} = \frac{\partial^2 \theta^{\mathrm{l}}}{\partial x^2}, \qquad 0 < x < s(t), \tag{2.8}$$

Nondimensional heat equation in solid region:

$$\frac{\partial \theta^{\mathrm{s}}}{\partial t} = \alpha \frac{\partial^2 \theta^{\mathrm{s}}}{\partial x^2}, \qquad x \geq s(t). \tag{2.9}$$

Nondimensional boundary conditions:

$$\begin{aligned} \theta^{\mathrm{l}}(x,t)\Big|_{x=0} &= 1, \\ \lim_{x\to\infty} \theta^{\mathrm{s}}(x,t) &= -1, \end{aligned} \tag{2.10}$$

Nondimensional interface condition:

$$\theta^{\mathrm{l}}(x,t)\Big|_{x=s(t)} = 0 = \theta^{\mathrm{s}}(x,t)\Big|_{x=s(t)}, \tag{2.11}$$

Nondimensional initial condition:

$$\theta^{\mathrm{s}}(x,t)\Big|_{t=0} = -1, \tag{2.12}$$

Nondimensional Stefan condition:

$$\frac{\mathrm{d}s}{\mathrm{d}t} = -\mathrm{Ste}^{\mathrm{l}} \frac{\partial \theta^{\mathrm{l}}}{\partial x}\bigg|_{x=s(t)} + \mathrm{Ste}^{\mathrm{s}} \frac{\partial \theta^{\mathrm{s}}}{\partial x}\bigg|_{x=s(t)}, \tag{2.13}$$

where $\alpha = \alpha^{\mathrm{s}}/\alpha^{\mathrm{l}}$ in (2.9) denotes the ratio of thermal diffusivities of the phases. Stefan numbers $\mathrm{Ste}^{\mathrm{l}} = c_p^{\mathrm{l}}(\theta_0 - \theta_{\mathrm{m}})/\mathrm{L}_{\mathrm{m}}$, $\mathrm{Ste}^{\mathrm{s}} = c_p^{\mathrm{s}}(\theta_{\mathrm{m}} - \theta_\infty)/\mathrm{L}_{\mathrm{m}}$ in (2.13) are the only characteristic numbers of the formulated nondimensional problem.

Analytic solution

Analytic solution using the similarity variable $\xi = x/\sqrt{t}$ is often attributed to J. von Neumann[ii]. Substitution of ξ to equation (2.8) and assuming that $\theta^{\mathrm{l}} = \theta^{\mathrm{l}}(\xi)$ reduces it to a second order linear ODE:

$$\frac{\mathrm{d}^2\theta^{\mathrm{l}}}{\mathrm{d}\xi^2} = -\frac{\xi}{2}\frac{\mathrm{d}\theta^{\mathrm{l}}}{\mathrm{d}\xi},$$

using substitution $\eta^{\mathrm{l}} = \partial\theta^{\mathrm{l}}/\partial\xi$, we get a first order linear ODE:

$$\frac{\partial\eta^{\mathrm{l}}}{\partial\xi} = -\frac{\xi}{2}\eta^{\mathrm{l}},$$

which after separation of variables yields a solution in the form:

$$\eta^{\mathrm{l}} = \frac{\mathrm{d}\theta^{\mathrm{l}}}{\mathrm{d}\xi} = C_0\mathrm{e}^{-(\xi/2)^2}.$$

This leads us to the conclusion that[iii]:

$$\theta^{\mathrm{l}}(x,t) = C_1\,\mathrm{erf}\left(\frac{x}{2\sqrt{t}}\right) + C_2. \tag{2.14}$$

By the same procedure we can solve the equation (2.9) to obtain the temperature distribution in the solid phase region:

$$\theta^{\mathrm{s}}(x,t) = C_3\,\mathrm{erf}\left(\frac{x}{2\sqrt{\alpha t}}\right) + C_4. \tag{2.15}$$

Now if we take into account the boundary and interface conditions (2.10)–(2.11):

$$\theta^{\mathrm{l}}(x,t)\Big|_{x=0} = C_2 = 1, \tag{2.16}$$

$$\theta^{\mathrm{l}}(x,t)\Big|_{x=s(t)} = C_1\,\mathrm{erf}\left(\frac{s(t)}{2\sqrt{t}}\right) + 1 = 0, \tag{2.17}$$

[ii] John von Neumann (1903–1957) – outstanding American mathematician, one of the leaders in the creation of the first computers.

[iii] Just as a reminder $\mathrm{erf}\,()$ is the error funtion defined as:

$$\mathrm{erf}\,(x) \coloneqq \frac{2}{\sqrt{\pi}}\int_0^x \mathrm{e}^{-t^2}\mathrm{d}t,$$

$\mathrm{erfc}\,()$ denotes the complementary error function:

$$\mathrm{erfc}\,(x) \coloneqq 1 - \mathrm{erf}\,(x) = \frac{2}{\sqrt{\pi}}\int_x^\infty \mathrm{e}^{-t^2}\mathrm{d}t.$$

for C_1 to be a constant, we need to assume that $s \propto \sqrt{t}$, therefore we set:

$$s(t) = 2\lambda\sqrt{t}, \tag{2.18}$$

which gives with (2.16) and (2.17) the nondimensional temperature distribution in the liquid subdomain:

$$\theta^{\mathrm{l}}(x,t) = -\frac{1}{\operatorname{erf}\lambda}\operatorname{erf}\left(\frac{x}{2\sqrt{t}}\right) + 1. \tag{2.19}$$

In a complete analogy, we can derive the nondimensional temperature distribution in the solid region:

$$\theta^{\mathrm{s}}(x,t) = \frac{1}{\operatorname{erfc}\left(\lambda/\sqrt{\alpha}\right)}\operatorname{erfc}\left(\frac{x}{2\sqrt{\alpha t}}\right) - 1. \tag{2.20}$$

The only remaining piece of information is that about λ. So far, we have not used the Stefan condition (2.13), which gives—after substitution of obtained solutions (2.19), (2.20)—the following transcendental equation:

$$\lambda = \mathrm{Ste}^{\mathrm{l}}\frac{\mathrm{e}^{-\lambda^2}}{\sqrt{\pi}\operatorname{erf}(\lambda)} - \mathrm{Ste}^{\mathrm{s}}\frac{\sqrt{\alpha}\,\mathrm{e}^{-\lambda^2/\alpha}}{\sqrt{\pi}\operatorname{erfc}\left(\lambda/\sqrt{\alpha}\right)}. \tag{2.21}$$

Such an equation can be solved using standard root finding procedures, e.g. Newton method. Next, we will show, that the root exists and it is unique. First, we set:

$$f(\lambda) \coloneqq \mathrm{Ste}^{\mathrm{l}}\frac{\mathrm{e}^{-\lambda^2}}{\sqrt{\pi}\operatorname{erf}(\lambda)} - \mathrm{Ste}^{\mathrm{s}}\frac{\sqrt{\alpha}\,\mathrm{e}^{-\lambda^2/\alpha}}{\sqrt{\pi}\operatorname{erfc}\left(\lambda/\sqrt{\alpha}\right)} - \lambda.$$

Obviously $f(\lambda)$ is a C^1 function for $\lambda \in (0,\infty)$. Moreover because $\lim_{\lambda\to 0^+}\operatorname{erf}\lambda = 0,\ \lim_{\lambda\to\infty}\operatorname{erf}\lambda = 1$, we can look for its limits at the end points:

$$\begin{aligned}
\lim_{\lambda\to 0^+} f(\lambda) &= \lim_{\lambda\to 0^+}\left(\mathrm{Ste}^{\mathrm{l}}\frac{\mathrm{e}^{-\lambda^2}}{\sqrt{\pi}\operatorname{erf}(\lambda)}\right) - \mathrm{Ste}^{\mathrm{s}}\frac{\sqrt{\alpha}}{\sqrt{\pi}} = \infty,\\
\lim_{\lambda\to\infty} f(\lambda) &= \lim_{\lambda\to\infty}\left(-\mathrm{Ste}^{\mathrm{s}}\frac{\sqrt{\alpha}\,\mathrm{e}^{-\lambda^2/\alpha}}{\sqrt{\pi}\operatorname{erfc}\left(\lambda/\sqrt{\alpha}\right)} - \lambda\right),\\
\lim_{\lambda\to\infty}\frac{\mathrm{e}^{-\lambda^2/\alpha}}{\operatorname{erfc}\left(\lambda/\sqrt{\alpha}\right)} &= \left[\frac{0}{0}\right] \overset{(\mathrm{H})}{=} \lim_{\lambda\to\infty}\frac{-2\lambda/\alpha\mathrm{e}^{-\lambda^2/\alpha}}{-2/\sqrt{\pi\alpha}\mathrm{e}^{-\lambda^2/\alpha}} = \lim_{\lambda\to\infty}\sqrt{\frac{\pi}{\alpha}}\lambda = \infty,
\end{aligned}$$

where (H) means that we used the l'Hôspital's rule—both the numerator and the denominator contain a function that is differentiable on $(0,\infty)$. So $f(\lambda)$ is a continuous function with $\lim_{\lambda\to 0^+} f(\lambda) = \infty$ and $\lim_{\lambda\to\infty} f(\lambda) = -\infty$. Applying Bolzano's theorem (or corollary of the Intermediate value theorem) we ensure existence of at least one root of funtion $f(\lambda)$. Let us further denote:

$$\begin{aligned}
f_1(\lambda) &= \mathrm{e}^{\lambda^2}\operatorname{erf}(\lambda),\\
f_2(\lambda) &= \mathrm{e}^{\lambda^2/\alpha}\operatorname{erfc}\left(\frac{\lambda}{\sqrt{\alpha}}\right),\\
f_3(\lambda) &= -\lambda,
\end{aligned}$$

than we immediately see, that $f_3(\lambda)$ is strictly decreasing on $(0,\infty)$. Further, we want to explore the monotonicity of the other two funtions, since both are smooth, we can differentiate, thus:

$$\frac{\mathrm{d}f_1}{\mathrm{d}\lambda} = 2\lambda \mathrm{e}^{\lambda^2}\operatorname{erf}(\lambda) + \mathrm{e}^{\lambda^2}\frac{2}{\sqrt{\pi}}\mathrm{e}^{-\lambda^2} > 0,\ \lambda \in (0,\infty)$$
$$\frac{\mathrm{d}f_2}{\mathrm{d}\lambda} = \frac{2\lambda}{\alpha}\mathrm{e}^{\lambda^2/\alpha}\operatorname{erfc}\left(\frac{\lambda}{\sqrt{\alpha}}\right) - \frac{2}{\sqrt{\pi\alpha}} =: g(\lambda).$$

Set $\phi(\lambda) \coloneqq \mathrm{e}^{-\lambda^2/\alpha}g(\lambda) = 2/\alpha\lambda\operatorname{erfc}(\lambda/\sqrt{\alpha}) - 2/\sqrt{\pi\alpha}\mathrm{e}^{-\lambda^2/\alpha}$, than obviously $\phi(0) < 0$, but also $\lim_{\lambda\to\infty}\phi(\lambda) = 0$, since:

$$\lim_{\lambda\to\infty}\lambda\operatorname{erfc}\lambda = \lim_{\lambda\to\infty}\frac{\operatorname{erfc}\lambda}{1/\lambda} = \left[\frac{0}{0}\right] \overset{\text{(H)}}{=} \lim_{\lambda\to\infty}\frac{2/\sqrt{\pi}\mathrm{e}^{-\lambda^2}}{-1/\lambda^2} = 0.$$

The last missing piece is that $\mathrm{d}/\mathrm{d}\lambda\,\phi(\lambda) > 0$, that is:

$$\begin{aligned}\frac{\mathrm{d}}{\mathrm{d}\lambda}\phi(\lambda) &= \frac{2}{\alpha}\operatorname{erfc}\left(\frac{\lambda}{\sqrt{\alpha}}\right) - \frac{2}{\alpha}\lambda\frac{2}{\sqrt{\pi\alpha}}\mathrm{e}^{-\lambda^2/\alpha} + \frac{4}{\sqrt{\pi\alpha}\alpha}\lambda\mathrm{e}^{-\lambda^2/\alpha} = \\ &= \frac{2}{\alpha}\operatorname{erfc}\left(\frac{\lambda}{\sqrt{\alpha}}\right) > 0,\ \lambda \in (0,\infty).\end{aligned}$$

We can conclude that $\phi(\lambda) < 0,\ \forall\lambda \in (0,\infty)$, therefore $0 > \mathrm{e}^{\lambda^2/\alpha}\phi(\lambda) = g(\lambda)$. This means that $f_2(\lambda)$ is strictly decreasing function on $(0,\infty)$. Finally:

$$f(\lambda) = \frac{\mathrm{Ste}^{\mathrm{l}}}{\sqrt{\pi}}\frac{1}{f_1(\lambda)} - \frac{\mathrm{Ste}^{\mathrm{s}}\sqrt{\alpha}}{\sqrt{\pi}}\frac{1}{f_2(\lambda)} + f_3(\lambda),$$

thus $f(\lambda)$ is a sum of strictly decreasing functions, hence it is strictly decreasing, meaning there is a unique root of the transcendental equation. This concludes our proof.

To summarize, analytical solution of our nondimensional two-phase Stefan problem on a semi-infinite homogeneous slab is given by:

Nondimensional solution in liquid region:

$$\theta^{\mathrm{l}}(x,t) = -\frac{1}{\operatorname{erf}\lambda}\operatorname{erf}\left(\frac{x}{2\sqrt{t}}\right) + 1, \qquad 0 < x < s(t),$$

Nondimensional solution in solid region:

$$\theta^{\mathrm{s}}(x,t) = \frac{1}{\operatorname{erfc}(\lambda/\sqrt{\alpha})}\operatorname{erfc}\left(\frac{x}{2\sqrt{\alpha t}}\right) - 1,\ \ x \geq s(t),$$

Position of the melting front:

$$s(t) = 2\lambda\sqrt{t},$$

Transcendental equation:

$$\lambda = \mathrm{Ste}^{\mathrm{l}}\frac{\mathrm{e}^{-\lambda^2}}{\sqrt{\pi}\operatorname{erf}(\lambda)} - \mathrm{Ste}^{\mathrm{s}}\frac{\sqrt{\alpha}\,\mathrm{e}^{-\lambda^2/\alpha}}{\sqrt{\pi}\operatorname{erfc}(\lambda/\sqrt{\alpha})}.$$

For the sake of completeness let us add the solution expressed in *dimensional* variables:

Solution in liquid region:

$$\theta^{\mathrm{l}}(x,t) = \theta_0 - (\theta_0 - \theta_{\mathrm{m}})\frac{1}{\operatorname{erf}\lambda}\operatorname{erf}\left(\frac{x}{2\sqrt{\alpha^{\mathrm{l}}\,t}}\right), \qquad 0 < x < s(t),$$

Solution in solid region:

$$\theta^{\mathrm{s}}(x,t) = \theta_\infty + (\theta_{\mathrm{m}} - \theta_\infty)\frac{1}{\operatorname{erfc}\left(\lambda/\sqrt{\alpha}\right)}\operatorname{erfc}\left(\frac{x}{2\sqrt{\alpha^{\mathrm{s}}\,t}}\right), \; x \geq s(t),$$

Position of the melting front:

$$s(t) = 2\lambda\sqrt{\alpha^{\mathrm{l}}\,t}.$$

2.1.2 Discrete problem

With respect to adopted assumptions, we will now formulate the discrete problem using Enthalpy method, which we will use then to state the problem weakly.

Weak formulation

This time, our domain of interest is finite—and of unitary length (see Figure 2.2), which gives rise to a question of the second boundary condition. Since our main goal is to benchmark the solution of the discrete problem with the analytical solution (2.18)–(2.20), the heat flux given by the analytical solution will be prescribed, i.e.:

$$q(t) \coloneqq -k^{\mathrm{s}}\frac{\partial\theta^{\mathrm{s}}(x,t)}{\partial x}\bigg|_{x=1} \overset{(2.20)}{=} -k^{\mathrm{s}}\frac{\mathrm{e}^{-1/(4\alpha t)}}{\sqrt{\pi\alpha t}\operatorname{erfc}\left(\lambda/\sqrt{\alpha}\right)}. \tag{2.22}$$

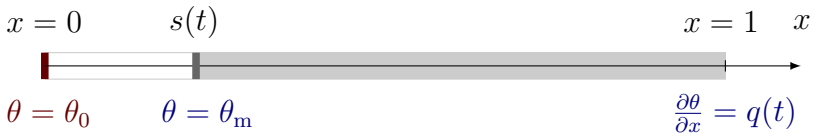

Figure 2.2: Formulation of the one-dimensional Stefan problem for a discretized solution. Heat flux through the left end of the bar $q(t)$ is given by the analytical solution.

The problem is again governed by the heat equation (2.1), but in the case of diffused-interface formulation it takes the form:

$$\rho\,(c_p)_\epsilon(\theta)\frac{\partial\theta}{\partial t} = \operatorname{div}\left(k_\epsilon(\theta)\frac{\partial\theta}{\partial x}\right). \tag{2.23}$$

As a general strategy, we will employ the Rothe method, first suggested by Erich Rothe in 1930. We therefore approximate the time derivative using finite time difference:

$$\frac{\partial\theta}{\partial t} \approx \frac{\theta^k - \theta^{k-1}}{\Delta t},$$

and assume that the solution is constant on the time interval of length Δt—with the given initial condition θ^{k-1}. Generally, we consider a convex combination of θ^k and θ^{k-1} to be substituted into the heat equation (2.23):

$$\rho\,(c_p)_\epsilon(\theta)\frac{\theta^k-\theta^{k-1}}{\Delta t}=\operatorname{div}\left(k_\epsilon(\theta)\frac{\partial\left(\Theta\theta^k+(1-\Theta)\theta^{k-1}\right)}{\partial x}\right), \tag{2.24}$$

which we solve with respect to θ^k, a function of the space only. For specific values of Θ we obtain either fully explicit ($\Theta=0$) or fully implicit ($\Theta=1$) scheme. For $\Theta=1/2$, we get the so-called *Crank-Nicolson scheme*. Fully implicit Euler scheme is the preferred one in this thesis. The complete discretised solution will be then given by:

$$\theta(x,t)=\theta^k(x);\ x\in(0,1), t\in(t^{k-1},t^k], \tag{2.25}$$

where $t^k=k\Delta t,\ k\in\{1,\dots,N\}$. Next, for a fixed time instant t^k, we define the elliptic problem (2.24), whose weak formulation we will now carefully derive.

First, let us consider the following vector space:

$$\mathcal{T}\coloneqq\{\vartheta\in H^1\left((0,1)\right)\mid\vartheta(0)=0\}^{\text{iv}}. \tag{2.26}$$

We see, that if we assume θ_0 to be a constant function on the unit interval, we can define $\mathcal{T}\ni\widetilde{\theta}^k\coloneqq\theta^k-\theta_0$. Multiplying the elliptic equation (2.24) with a test function $\vartheta\in\mathcal{T}$ and integrating over the unit interval we obtain the following integral identity:

$$\rho\int_0^1 c_p^\varepsilon\frac{\theta^k-\theta^{k-1}}{\Delta t}\vartheta\,\mathrm{d}x=\int_0^1\operatorname{div}\left(k^\varepsilon\frac{\partial\theta}{\partial x}\right)\vartheta\,\mathrm{d}x.$$

It only remains to apply the Green's first identity[v]—not forgetting the Neumann boundary condition (2.22)—and we obtain the *weak formulation* of the problem:

At $t=t^k$ we look for $\widetilde{\theta}^k\in\mathcal{T}$, such that:

$$\rho\int_0^1 c_p^\varepsilon\frac{\widetilde{\theta}^k}{\Delta t}\vartheta\mathrm{d}x+\int_0^1 k^\varepsilon\frac{\partial\widetilde{\theta}^k}{\partial x}\frac{\partial\vartheta}{\partial x}\mathrm{d}x=\rho\int_0^1 c_p^\varepsilon\frac{\widetilde{\theta}^{k-1}}{\Delta t}\vartheta\mathrm{d}x+ \\ +q(t^k)\vartheta(1),\ \forall\vartheta\in\mathcal{T}. \tag{2.27}$$

Existence and uniqueness of a solution of this problem is given by the well known *Lax-Milgram lemma*.

[iv] Here we use the continuous representative ϑ, since $H^1\left((0,1)\right)=AC\left((0,1)\right)$ in the sense, that: $\forall\vartheta\in H^1\left((0,1)\right)\exists\tilde{\vartheta}\in AC\left((0,1)\right):\ \vartheta=\tilde{\vartheta}$ a.e., so $\vartheta(0)$ has a meaning.

[v] Let $u,\,v\in H^1(\omega)$ be two Sobolev functions on a domain with Lipschitz boundary, then:

$$\int_\omega u\frac{\partial v}{\partial x_i}\mathrm{d}\mathbf{x}=\oint_{\partial\omega}uvn_i\mathrm{d}S-\int_\omega\frac{\partial u}{\partial x_i}v\mathrm{d}\mathbf{x},$$

where n_i denotes the i-th component of an outer normal on $\partial\omega$ and the derivatives are meant in the weak sense.

FEM solution

The variational problem (2.27) was implemented numerically in the open-source platform FEniCS. The temperature was discretised using linear finite elements and solution of the transcendental equation (2.21) was sought using root finding procedure `fsolve` from the `scipy.optimize` package. Table 2.1 gives numerical values of the material parameters for the simulation and boundary condition values.

	Parameter	Value
Material quantity	ρ	$1000\,\mathrm{kg/m^3}$
	c_p^{l}	$4180\,\mathrm{J\,kg^{-1}\,K^{-1}}$
	c_p^{s}	$2050\,\mathrm{J\,kg^{-1}\,K^{-1}}$
	k^{l}	$0.571\,\mathrm{W\,m^{-1}\,K^{-1}}$
	k^{s}	$2.18\,\mathrm{W\,m^{-1}\,K^{-1}}$
	$\mathrm{L_m}$	$334 \cdot 10^3\,\mathrm{J/K}$
Formulation/discretisation	θ_0	$373\,\mathrm{K}$
	θ_{m}	$273\,\mathrm{K}$
	θ_∞	$263\,\mathrm{K}$
	x_{div}	1000
	Δt	$10^{-5}[\theta] \approx 730\,\mathrm{s}$
	ϵ	$0.4\,\mathrm{K}$

Table 2.1: Numerical values of parameters of one-dimensional Stefan problem.

2.1.3 Results

Figure 2.3 shows the accuracy of the proposed enthalpy method on a benchmarking code comparing it with the analytic solution of the Stefan problem. A remarkable agreement in both the melting front position and the temperature distribution is present.

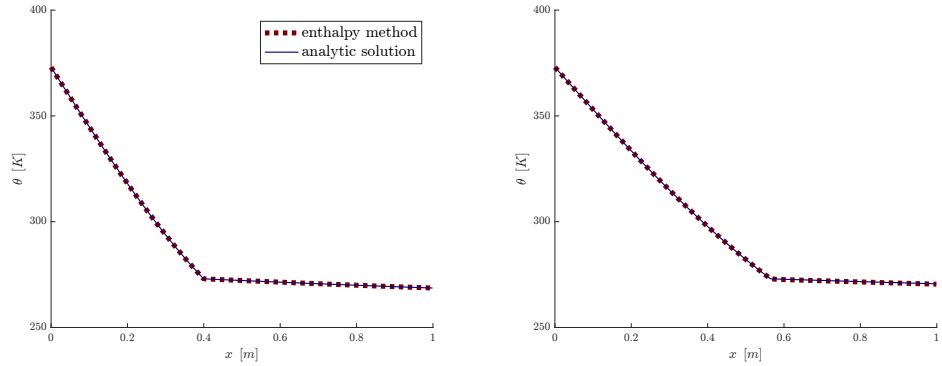

(a) $t = 10^{-1}[t] \approx 7.3 \cdot 10^5$ s - the initial value.

(b) $t = 2 \cdot 10^{-1}[t]$

(c) $t = 3 \cdot 10^{-1}[t]$

(d) $t = 4 \cdot 10^{-1}[t]$

(e) $t = 5 \cdot 10^{-1}[t]$

(f) $t = 6 \cdot 10^{-1}[t]$

Figure 2.3: Benchmarking of the enhalpy method with the analytical solution of the one-dimensional Stefan problem.

Stability

With particular combination of mesh cell size Δx, time step size Δt and mollifying parameter ϵ, the computation becomes unstable. What follows is an attempt to characterize the stability using a condition similar to established CFL condition, that is used as a stability criterion in many CFD computations.

First, it is necessary to discern the approximation of Dirac delta distribution within a discretisation of the temperature field. But what is possible is only to

control the domain discretization. Using integration by substitution we can write:

$$f(\theta_{\mathrm{m}}) = \int_{\mathbb{R}} f(\theta)\delta(\theta - \theta_{\mathrm{m}})\mathrm{d}\theta = \int_{\mathbb{R}} f(\theta(x))\delta(\theta(x) - \theta_{\mathrm{m}})\frac{\mathrm{d}\theta}{\mathrm{d}x}\mathrm{d}x,$$

and consequently we can write for Δx:

$$\Delta x \leq \epsilon_x \approx \epsilon \left(\frac{\mathrm{d}\theta}{\mathrm{d}x}\right)^{-1} \approx \epsilon \frac{[x]}{\theta_0 - \theta_\infty},$$

where ϵ_x denotes the mollification width with respect to spatial metric. In a complete analogy to the CFL condition we would like to bound the time step size using a characteristic information distribution velocity. In the case of Stefan problem, the characteristic property is the melting front position. Its order of magnitude is given by the Stefan condition (2.7):

$$\rho \mathrm{L}_{\mathrm{m}} \frac{\mathrm{d}s}{\mathrm{d}t} \approx -k^{\mathrm{l}} \frac{\theta_0 - \theta_\infty}{[x]} + k^{\mathrm{s}} \frac{\theta_0 - \theta_\infty}{[x]} \leq (k^{\mathrm{l}} + k^{\mathrm{s}}) \frac{\theta_0 - \theta_\infty}{[x]}.$$

It is now only a matter of a standard requirement, that the time step size should be small enough to be able to contain the propagating information within consecutive mesh cells after one time step, i.e.:

$$\Delta \tilde{t} = \frac{\Delta t}{[t]} \leq \frac{\Delta x}{[t]\mathrm{d}s/\mathrm{d}t} \leq \epsilon \frac{[x]}{\theta_0 - \theta_\infty} \frac{k^{\mathrm{l}}}{[x]^2 \rho c_p^{\mathrm{l}}} \frac{\rho \mathrm{L}_{\mathrm{m}}[x]}{(\theta_0 - \theta_\infty)(k^{\mathrm{l}} + k^{\mathrm{s}})} \approx \frac{\epsilon \mathrm{L}_{\mathrm{m}}}{(\theta_0 - \theta_\infty)^2 c_p^{\mathrm{l}}}.$$

Let us see what this criterion gives for our problem settings. We fix $\epsilon = 0.1$ and from Table 2.1 we see that:

$$\begin{aligned}
\Delta x &\leq \epsilon \frac{[x]}{\theta_0 - \theta_\infty} \approx 10^{-1} \frac{1}{10^2} = 10^{-3}, \\
\Delta \tilde{t} &\leq \frac{\epsilon \mathrm{L}_{\mathrm{m}}}{(\theta_0 - \theta_\infty)^2 c_p^{\mathrm{l}}} \approx \frac{10^{-1} \cdot 10^5}{10^4 \cdot 10^3} = 10^{-3}, \\
\Delta \tilde{t} &\leq \frac{\Delta x}{[t]\mathrm{d}s/\mathrm{d}t} \leq \Delta x \frac{\mathrm{L}_{\mathrm{m}}}{[x] c_p^{\mathrm{l}} (\theta_0 - \theta_\infty)} \approx \Delta x \frac{10^{-5}}{1 \cdot 10^3 \cdot 10^2} = \Delta x.
\end{aligned} \tag{2.28}$$

Numbers $\epsilon = 10^{-1}$, $\Delta x = 10^{-3}$ and $\Delta \tilde{t} = 10^{-3}$ give an upper bound for stability of the computation. Figure 2.4 depicts result of a numerical experiment, that shows the relation between an error—expressed by the difference of a position of the melting front given by analytic vs. discrete solution.

It is obvious, that if we respect bounds given by the previous calculations, the computation gives meaningful results. Outside the safe region the resulting temperature fields may give non-physical description of the problem—depicted by red patches in Figure 2.4.

2.2 Stefan 2D

It is noteworthy that the heat equation formulated as a radially symmetric planar problem retains the structure suitable for definition of the same similarity variable $\xi = r/\sqrt{t}$.

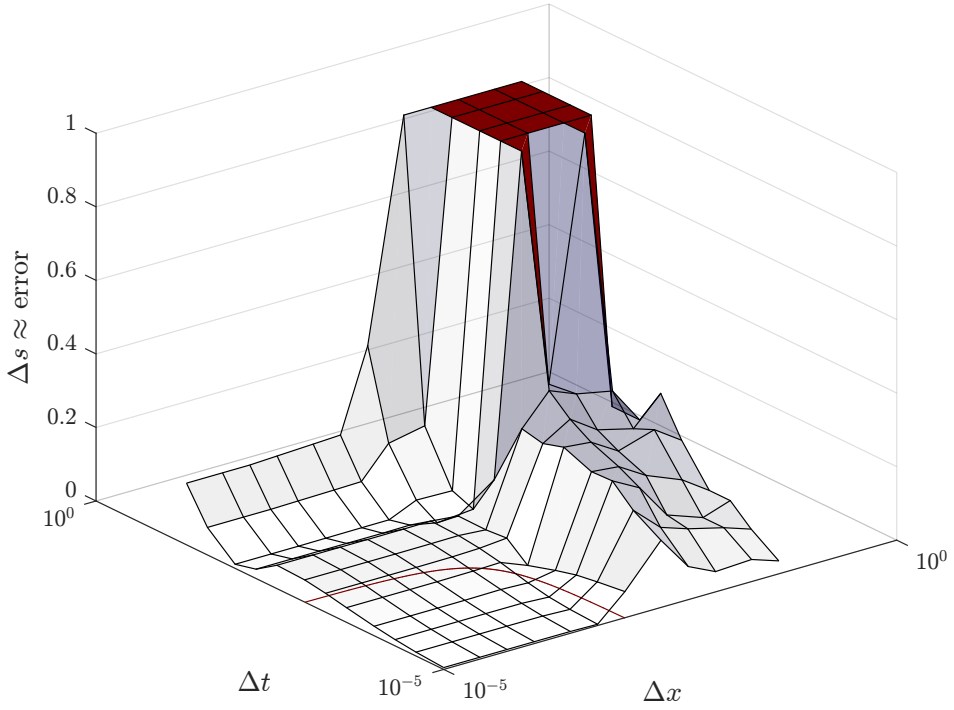

Figure 2.4: Stability of Stefan 1D problem. z-axis shows an error that is given by the difference of the position of the melting front. Red curve in the $\Delta x - \Delta t$ plane shows restriction on the time step size (2.28), $\Delta s = 1$ means that no melting front position was given by the calculation using the particular choice of parameters—computation became unstable.

2.2.1 Continuous problem

Formulation

An infinite plane of a constant thickness with excluded circular region of radius $r = R_1$ is centered at the origin is the domain of interest. Graphic interpretation of the formulation is contained in Figure 2.5.

In a complete analogy to the one-dimensional case we assume the following:

- The material is thermally insulated so that no heat escapes through the upper and lower boundary of the disc.
- There are no heat sources within the material.

The rest of the formulation can be adopted from the section Stefan 1D, the only difference is that now we don't prescribe temperature on the boundary (inner circle), but the heat flux. The reason for this as well as for the shape of the domain will be clear from the analytical solution of the problem. Radial symmetry of the problem gives the dependence of the temperature only on r spatial coordinate, therefore $\theta = \theta(r, t)$.

Our starting point is the heat equation in an invariant form (2.1), Table 2 of Appendix B contains differential operators in cylindrical coordinates. Using

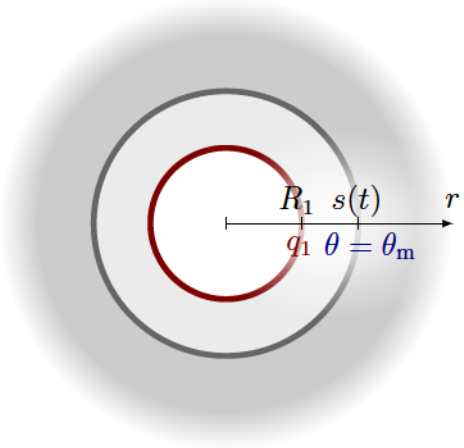

Figure 2.5: Sharp-interface formulation of the two-dimensional Stefan problem. Here we prescribe Neumann boundary condition $-k^\mathrm{l}\partial\theta^\mathrm{l}/\partial r|_{r=R_1} = q_1$.

the definition of a laplacian we can write:

$$\rho c_p \frac{\partial \theta}{\partial t} = \operatorname{div}(k\nabla\theta) = k\Delta\theta = k\frac{1}{r}\frac{\partial}{\partial r}\left(r\frac{\partial\theta}{\partial r}\right) = k\left(\frac{\partial^2\theta}{\partial r^2} + \frac{1}{r}\frac{\partial\theta}{\partial r}\right). \tag{2.29}$$

It remains to observe that the Stefan condition (2.7) retains its structure in the polar coordinates. We denote $\mathbf{s} = (s_r, s_\varphi)$ the position of the melting front expressed in polar coordinates, then it holds:

$$\begin{aligned}\rho \mathrm{L_m}\frac{\mathrm{d}\mathbf{s}}{\mathrm{d}t}\cdot\mathbf{n}_\sigma = -[\![\mathbf{q}]\!]\cdot\mathbf{n}_\sigma = k^\mathrm{s}\nabla\theta^\mathrm{s}\cdot\mathbf{n}_\sigma - k^\mathrm{l}\nabla\theta^\mathrm{l}\cdot\mathbf{n}_\sigma = \\ = k^\mathrm{s}\frac{\partial\theta^\mathrm{s}}{\partial r}\mathbf{e}_{\hat{r}}\cdot\mathbf{n}_\sigma - k^\mathrm{l}\frac{\partial\theta^\mathrm{l}}{\partial r}\mathbf{e}_{\hat{r}}\cdot\mathbf{n}_\sigma,\end{aligned}$$

where $\mathbf{e}_{\hat{r}}$ is the unit basis vector in the radial direction. Because we assume, that the problem possesses cylindrical symmetry, it holds that $\mathbf{n}_\sigma = \mathbf{e}_{\hat{r}}$ and we can write the final form of the Stefan condition:

$$\rho \mathrm{L_m}\frac{\mathrm{d}s_r}{\mathrm{d}t} = -k^\mathrm{l}\left.\frac{\partial\theta^\mathrm{l}}{\partial r}\right|_{r=s_r(t)} + k^\mathrm{s}\left.\frac{\partial\theta^\mathrm{s}}{\partial r}\right|_{r=s_r(t)}.$$

Formulation of the two-dimensional Stefan problem:

Heat equation in liquid region:

$$\frac{\partial \theta^{\mathrm{l}}}{\partial t} = \alpha^{\mathrm{l}} \left(\frac{\partial^2 \theta^{\mathrm{l}}}{\partial r^2} + \frac{1}{r} \frac{\partial \theta^{\mathrm{l}}}{\partial r} \right), \qquad R_1 < r < s_r(t), \tag{2.30}$$

Heat equation in solid region:

$$\frac{\partial \theta^{\mathrm{s}}}{\partial t} = \alpha^{\mathrm{s}} \left(\frac{\partial^2 \theta^{\mathrm{s}}}{\partial r^2} + \frac{1}{r} \frac{\partial \theta^{\mathrm{s}}}{\partial r} \right), \qquad r \geq s_r(t). \tag{2.31}$$

Boundary conditions:

$$\begin{aligned} -k^{\mathrm{l}} \frac{\partial \theta^{\mathrm{l}}}{\partial r}\Big|_{r=R_1} &= q_1, \\ \lim_{r \to \infty} \theta^{\mathrm{s}}(r,t) &= \theta_\infty, \end{aligned} \tag{2.32}$$

Interface condition:

$$\theta^{\mathrm{l}}(r,t)\Big|_{r=s_r(t)} = \theta_{\mathrm{m}} = \theta^{\mathrm{s}}(r,t)\Big|_{r=s_r(t)}, \tag{2.33}$$

Initial condition:

$$\theta^{\mathrm{s}}(x,t)\Big|_{t=0} = \theta_\infty, \tag{2.34}$$

Stefan condition:

$$\rho \mathrm{L}_{\mathrm{m}} \frac{\mathrm{d}s_r}{\mathrm{d}t} = -k^{\mathrm{l}} \frac{\partial \theta^{\mathrm{l}}}{\partial r}\bigg|_{r=s_r(t)} + k^{\mathrm{s}} \frac{\partial \theta^{\mathrm{s}}}{\partial r}\bigg|_{r=s_r(t)}.$$

Analytic solution

As was mentioned earlier in this section, the form of the polar heat equation (2.29) enables us to use practically the same procedure that led to the analytic solution of the one-dimensional case. Here we will consider general setting of the problem and with θ^{l} being function only of the r spatial coordinate—for both 2D and 3D formulation (as will be clarified in the next section)—we can formulate the heat equation using similarity variable ξ, that is:

$$\frac{\mathrm{d}^2 \theta^{\mathrm{l}}}{\mathrm{d}\xi^2} + \left(\frac{d-1}{\xi} + \frac{\xi}{2\alpha^{\mathrm{l}}} \right) \frac{\mathrm{d}\theta^{\mathrm{l}}}{\mathrm{d}\xi} = 0,$$

where d denotes the dimension of the space we solve the problem in. Using substitution $\eta^{\mathrm{l}} = \mathrm{d}\theta^{\mathrm{l}}/\mathrm{d}\xi$, we get a first order linear ODE:

$$\frac{\mathrm{d}\eta^{\mathrm{l}}}{\mathrm{d}\xi} + \left(\frac{d-1}{\xi} + \frac{\xi}{2\alpha^{\mathrm{l}}} \right) \eta^{\mathrm{l}} = 0,$$

or equivalently:

$$\frac{\mathrm{d}\eta^{\mathrm{l}}}{\eta^{\mathrm{l}}} + \left(\frac{d-1}{\xi} + \frac{\xi}{2\alpha^{\mathrm{l}}} \right) \mathrm{d}\xi, \tag{2.35}$$

which yields after integration:

$$\eta^{\mathrm{l}} = \frac{\mathrm{d}\theta^{\mathrm{l}}}{\mathrm{d}\xi} = C_0 \frac{1}{\xi^{d-1}} \, \mathrm{e}^{-\xi^2/(4\alpha^{\mathrm{l}})}.$$

Now if we integrate once more and apply substitution for the integral we obtain the general solution of the original ODE:

$$\theta^{\mathrm{l}}(r,t) = C_1 \int_{r^2/(4\alpha^{\mathrm{l}}t)}^{\infty} \frac{1}{t^{d/2}}\,\mathrm{e}^{-t}\,\mathrm{d}t + C_2 = C_1\Gamma\left(1-\frac{d}{2},\frac{r^2}{4\alpha^{\mathrm{l}}t}\right) + C_2, \tag{2.36}$$

where $\Gamma(s,x)$ denotes the incomplete gamma function[vi]. The same equation can be derived for the solid subdomain. For $d = 2$[vii] takes the incomplete gamma function the form of so-called exponential integral $\mathrm{Ei}(x)$[viii] and thus:

$$\theta^{\mathrm{l}}(r,t) = C_1 + C_2\,\mathrm{Ei}\left(-\frac{r^2}{4\alpha^{\mathrm{l}}t}\right),$$
$$\theta^{\mathrm{s}}(r,t) = C_3 + C_4\,\mathrm{Ei}\left(-\frac{r^2}{4\alpha^{\mathrm{s}}t}\right).$$

Since $\lim_{x\to 0^+}\mathrm{Ei}\,(x) = -\infty$, the solution θ^{l} would lack a physical meaning at $r = 0$. This is the reason why we solve the problem on $r \in [R_1,\infty)$ and therefore it is required to choose the constant C_2 in accordance with the heat flux q_1, i.e. $q_1 = -k^{\mathrm{l}}\partial\theta^{\mathrm{l}}/\partial r|_{r=R_1} = -k^{\mathrm{l}}C_2\,\mathrm{e}^{-(R_1^2/(4\alpha^{\mathrm{l}}t))}\,2/R_1 \to C_{q_1} := -q_1R_1\,\mathrm{e}^{(R_1^2/(4\alpha^{\mathrm{l}}t))}/(2k^{\mathrm{l}})$. After taking into consideration the data (2.44)–(2.46), we obtain the (dimensional) solution:

Solution in the liquid region:

$$\theta^{\mathrm{l}}(r,t) = \theta_{\mathrm{m}} - C_{q_1}\,\mathrm{Ei}\left(-\frac{\lambda^2}{\alpha^{\mathrm{l}}}\right) + C_{q_1}\,\mathrm{Ei}\left(-\frac{r^2}{4\alpha^{\mathrm{l}}t}\right), \quad R_1 < r < s_r(t), \tag{2.37}$$

Solution in the solid region:

$$\theta^{\mathrm{s}}(r,t) = \theta_\infty + (\theta_\infty - \theta_{\mathrm{m}})\frac{1}{\mathrm{Ei}\,(-\lambda^2/\alpha^{\mathrm{s}})}\,\mathrm{Ei}\left(-\frac{r^2}{4\alpha^{\mathrm{s}}t}\right),\ r \geq s_r(t), \tag{2.38}$$

Radius of the circular melting front:

$$s_r(t) = 2\lambda\sqrt{t},$$

Transcendental equation:

$$\rho\mathrm{L}_{\mathrm{m}}\lambda^2 = -k^{\mathrm{l}}\,\mathrm{e}^{-\lambda^2/\alpha^{\mathrm{l}}} - k^{\mathrm{s}}(\theta_\infty - \theta_{\mathrm{m}})\frac{\mathrm{e}^{-\lambda^2/\alpha^{\mathrm{s}}}}{\mathrm{Ei}\,(-\lambda^2/\alpha^{\mathrm{s}})}. \tag{2.39}$$

2.2.2 Discrete problem

For the discrete formulation our domain of interest changes into an annulus defined by radii R_1 and R_2. Heat fluxes through the boundary of the domain are

[vi] Definition of the upper incomplete gamma function:

$$\Gamma(s,x) := \int_x^{\infty} t^{s-1}\,\mathrm{e}^{-t}\,\mathrm{d}t.$$

[vii] If we had plugged $d = 1$ into (2.35), we would have gotten after integration the physical solution of the one-dimensional Stefan problem.

[viii] $\mathrm{Ei}\,()$ denotes the exponential integral:

$$\mathrm{Ei}(x) := -\int_{-x}^{\infty} \frac{1}{t}\,\mathrm{e}^{-t}\,\mathrm{d}t.$$

given by the analytic solution (2.37)–(2.38):

$$q_1(t) := -\frac{2k^{\mathrm{l}}C_{q_1}}{R_1}\,\mathrm{e}^{-R_1^2/(4\alpha^{\mathrm{l}}t)},$$
$$q_2(t) := -\frac{2k^{\mathrm{s}}(\theta_\infty - \theta_{\mathrm{m}})}{R_2\,\mathrm{Ei}\,(\lambda^2/\alpha^{\mathrm{s}})}\,\mathrm{e}^{-R_2^2/(4\alpha^{\mathrm{s}}t)}\,.$$

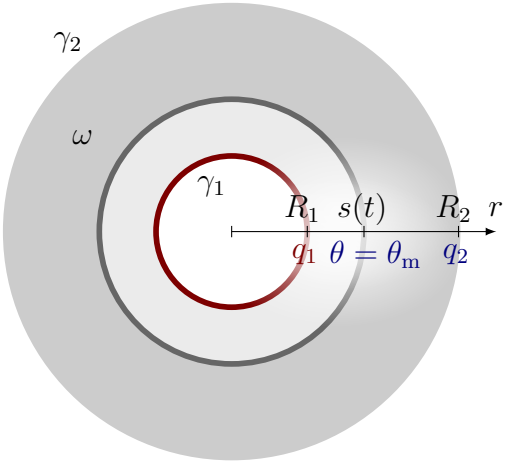

Figure 2.6: Discrete formulation of the two-dimensional Stefan problem using enthalpy method. Inner and outer boundary are denoted by γ_1, resp. γ_2.

Weak formulation

Repeating the procedure in the paragraph Weak formulation of the previous section, we obtain the variational formulation of the planar Stefan problem:

$$\begin{aligned}\text{At } t = t^k \text{ we look for } \theta^k \in H^1(\omega), \text{ such that:}\\ \rho\int_\omega c_p^\varepsilon \frac{\theta^k}{\Delta t}\vartheta\,\mathrm{d}\mathbf{x} + \int_\omega k^\varepsilon \nabla\theta^k\cdot\nabla\vartheta\,\mathrm{d}\mathbf{x} = \rho\int_\omega c_p^\varepsilon\frac{\theta^{k-1}}{\Delta t}\vartheta\mathrm{d}\mathbf{x} + \\ + \int_{\gamma_1} q_1(t^k)\vartheta\mathrm{d}S + \int_{\gamma_2} q_2(t^k)\vartheta\mathrm{d}S,\ \forall\vartheta\in H^1(\omega).\end{aligned} \tag{2.40}$$

FEM solution

As previously, the weak formulation (2.40) was implemented and solved numerically. The mesh of the domain was generated by `mshr` FEniCS library. Values of the material parameters are given by both the Table 2.1 and the following Table 2.2.

2.2.3 Results

Figure 2.7 makes a summary of benchmarking of the 2D enthalpy method vs. the analytical solution of the planar cylindrically symmetric Stefan problem. The result is, again, very satisfactory.

	Parameter	Value
Geometry	R_1	0.1 m
	R_2	1 m
Formulation/discretisation	C_{q_1}	100
	Δt	475 s

Table 2.2: Numerical values of parameters for two-dimensional cylindrically symmetric Stefan problem.

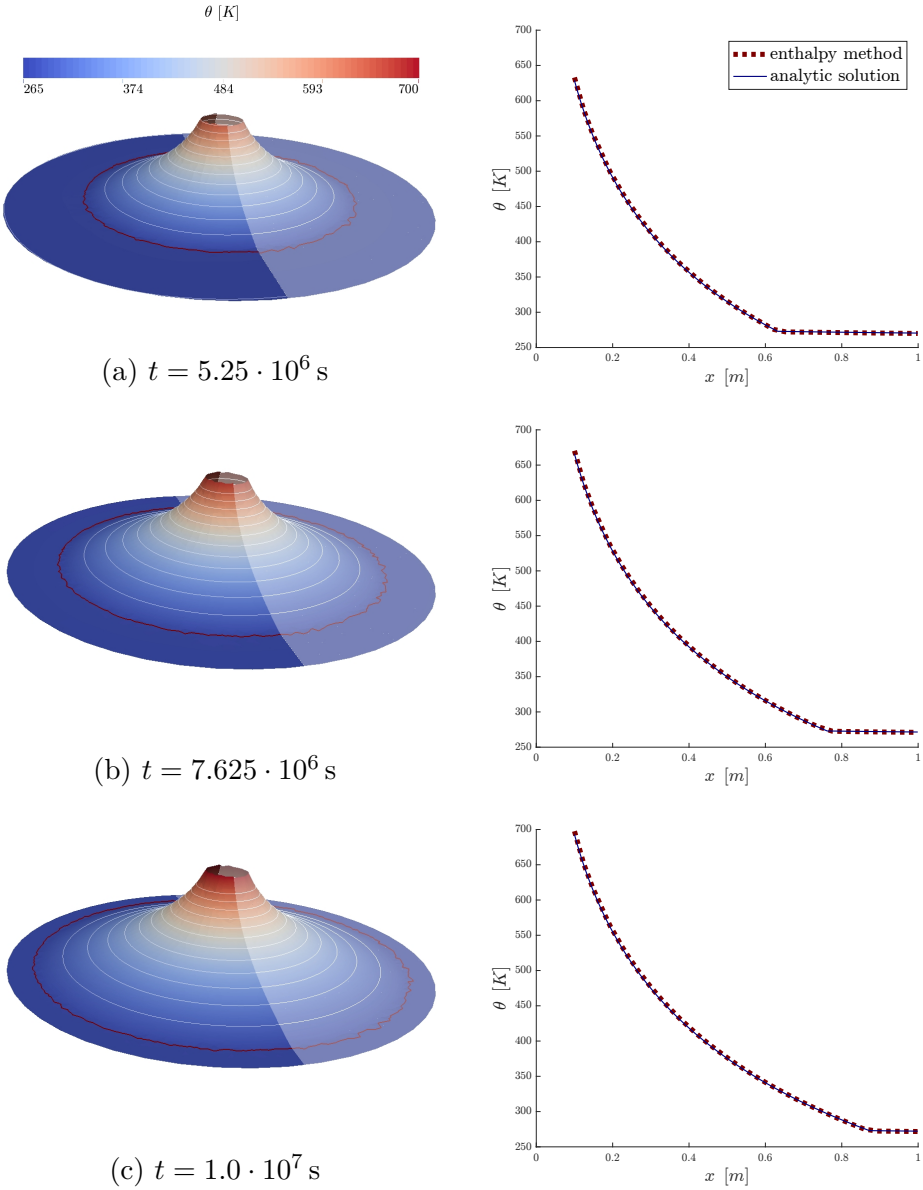

(a) $t = 5.25 \cdot 10^6$ s

(b) $t = 7.625 \cdot 10^6$ s

(c) $t = 1.0 \cdot 10^7$ s

Figure 2.7: Benchmarking of the enhalpy method with the analytical solution of the planar Stefan problem. The left column shows an attempt to represent temperature distribution on the annulus—left half being the FEM solution, right one, translucent, the analytic solution. White lines denotes temperature isolines, with the red one reserved for the melting front. The right column shows the comparison along one radial ray.

2.3 Stefan 3D

For the sake of completeness we present here the formulation and analytic solution of the three-dimensional radially symmetric Stefan problem. As the main focus of the thesis is aimed at the planar problems, discrete formulation and FEM solution of the spatial problem would not only be time consuming but also unjustified.

2.3.1 Continuous problem

Formulation

Formulation of the three-dimensional radially symmetric Stefan problem can be carried out in a complete analogy to the planar case. Figure 2.5 can be viewed as a cross section of the spherical domain. The heat equation (2.1) for $\theta = \theta(r,t)$ takes the form:

$$\rho c_p \frac{\partial \theta}{\partial t} = k \frac{1}{r^2} \frac{\partial}{\partial r} \left(r^2 \frac{\partial \theta}{\partial r} \right) = k \left(\frac{\partial^2 \theta}{\partial r^2} + \frac{2}{r} \frac{\partial \theta}{\partial r} \right). \tag{2.41}$$

Formulation of the spatial Stefan problem:

Heat equation in liquid region:

$$\frac{\partial \theta^{\mathrm{l}}}{\partial t} = \alpha^{\mathrm{l}} \left(\frac{\partial^2 \theta^{\mathrm{l}}}{\partial r^2} + \frac{2}{r} \frac{\partial \theta^{\mathrm{l}}}{\partial r} \right), \qquad R_1 < r < s_r(t), \tag{2.42}$$

Heat equation in solid region:

$$\frac{\partial \theta^{\mathrm{s}}}{\partial t} = \alpha^{\mathrm{s}} \left(\frac{\partial^2 \theta^{\mathrm{s}}}{\partial r^2} + \frac{2}{r} \frac{\partial \theta^{\mathrm{s}}}{\partial r} \right), \qquad r \geq s_r(t). \tag{2.43}$$

Boundary conditions:

$$\begin{aligned} -k^{\mathrm{l}} \frac{\partial \theta^{\mathrm{l}}}{\partial r}\Big|_{r=R_1} &= q_1, \\ \lim_{r \to \infty} \theta^{\mathrm{s}}(r,t) &= \theta_\infty, \end{aligned} \tag{2.44}$$

Interface condition:

$$\theta^{\mathrm{l}}(r,t)\Big|_{r=s_r(t)} = \theta_{\mathrm{m}} = \theta^{\mathrm{s}}(r,t)\Big|_{r=s_r(t)}, \tag{2.45}$$

Initial condition:

$$\theta^{\mathrm{s}}(x,t)\Big|_{t=0} = \theta_\infty, \tag{2.46}$$

Stefan condition:

$$\rho \mathrm{L}_{\mathrm{m}} \frac{\mathrm{d}s_r}{\mathrm{d}t} = -k^{\mathrm{l}} \frac{\partial \theta^{\mathrm{l}}}{\partial r}\bigg|_{r=s_r(t)} + k^{\mathrm{s}} \frac{\partial \theta^{\mathrm{s}}}{\partial r}\bigg|_{r=s_r(t)}.$$

Analytic solution

If we set $d = 3$ in (2.36) we obtain the general solution for the three-dimensional radially symmetric Stefan problem:

$$\theta^{\mathrm{l}}(r,t) = C_1 + C_2\,\Gamma\left(-\frac{1}{2}, \frac{r^2}{4\alpha^{\mathrm{l}}t}\right),$$
$$\theta^{\mathrm{s}}(r,t) = C_3 + C_4\,\Gamma\left(-\frac{1}{2}, \frac{r^2}{4\alpha^{\mathrm{s}}t}\right).$$

Taking into account the boundary conditions, we can write the particular solution:

Solution in the liquid region:

$$\theta^{\mathrm{l}}(r,t) = \theta_{\mathrm{m}} - C_{q_1}\Gamma\left(-\frac{1}{2}, \frac{\lambda^2}{\alpha^{\mathrm{l}}}\right) + C_{q_1}\Gamma\left(-\frac{1}{2}, \frac{r^2}{4\alpha^{\mathrm{l}}t}\right), \qquad R_1 < r < s_r(t),$$

Solution in the solid region:

$$\theta^{\mathrm{s}}(r,t) = \theta_\infty + (\theta_\infty - \theta_{\mathrm{m}})\frac{1}{\Gamma(-1/2, -\lambda^2/\alpha^{\mathrm{s}})}\Gamma\left(-\frac{1}{2}, \frac{r^2}{4\alpha^{\mathrm{s}}t}\right), \qquad r \geq s_r(t),$$

Radius of the circular melting front:

$$s_r(t) = 2\lambda\sqrt{t},$$

Transcendental equation:

$$\rho \mathrm{L}_{\mathrm{m}}\lambda^4 = -k^{\mathrm{l}}(\alpha^{\mathrm{l}})^{3/2}C_{q_1}\,\mathrm{e}^{-\lambda^2/\alpha^{\mathrm{l}}} - k^{\mathrm{s}}(\theta_\infty - \theta_{\mathrm{m}})(\alpha^{\mathrm{s}})^{3/2}\frac{\mathrm{e}^{-\lambda^2/\alpha^{\mathrm{s}}}}{\Gamma(-1/2, \lambda^2/\alpha^{\mathrm{s}})}.$$

3. Blankenbach benchmark

The present chapter is devoted to the second possible hindrance mentioned in Geometry and boundary conditions, that is the free surface. There are more ways how to deal with this boundary condition, nevertheless in view of fluid mechanics, the optimal one—and also the one we chose—is the so called *arbitrary Lagrangian-Eulerian* description of the problem. It enables us to stay within the advantageous framework of Eulerian description but at the same time gives the possibility to adapt the spatial discretisation to the time-dependent domain.

As in the case of the enthalpy method, we need to validate this approach. To this end we make use of the so-called Blankenbach benchmark, which contains a comparison study for thermal convection in the Earth's mantle. In the following we will present a formulation of a benchmark problem and a correlation of results for both fixed domain solution and the free surface problem—attacked by ALE formulation approach—complete with reference values given in [Blankenbach et al., 1989].

3.1 Fixed domain

3.1.1 Problem formulation

The benchmark problem is defined as a two-dimensional thermal convection of a non-rotating Boussinesq fluid of infinite Prandtl number in a rectangular cell of length l and height h, therefore $\omega := ((0, l) \times (0, h))$. The convection is driven by a horizontal temperature difference $\Delta\theta = \theta_{\text{bot}} - \theta_{\text{top}}$. Side walls of the cell are assumed to be thermally insulated and the fluid is allowed to slip freely on the whole boundary. Graphic representation of the formulation is available in Figure 3.1.

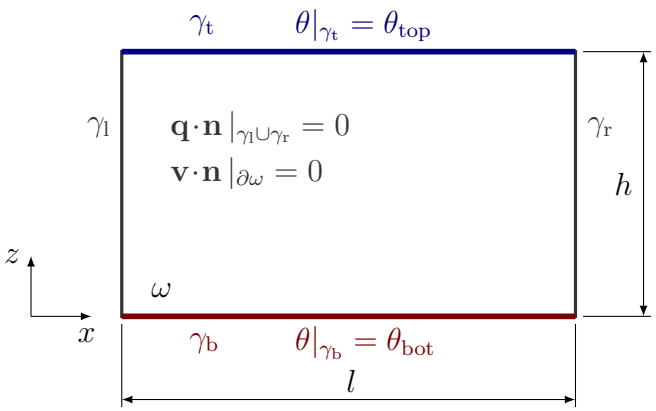

Figure 3.1: Formulation of the Blankenbach benchmark model problem.

3.1.2 Governing equations

The general approach in derivation of the governing equations consists in the linear approximation of the conservation laws called the *Oberbeck-Boussinesq*[i] *approximation.*

Oberbeck-Boussinesq approximation

Initially, we consider a hydrostatic reference state with $\mathbf{v} = \mathbf{0}$. The state is characterised by a reference pressure p_0^{th}, density ρ_0, temperature θ_0 and a reference gravitational constant $\mathbf{g}_0$. In the context of geophysical applications we assume a certain form of momentum equations (1.9), in particular those, that take into acount the rotation of the frame of reference:

$$\rho \frac{\mathrm{D}\mathbf{v}}{\mathrm{D}t} = \operatorname{div} \mathbb{T} + \rho \mathbf{g} - 2\rho\, \boldsymbol{\Omega} \times \mathbf{v} - \rho\, \boldsymbol{\Omega} \times (\boldsymbol{\Omega} \times \mathbf{x}) \quad \text{in } \omega, \tag{3.1}$$

where $\mathbf{x}$ is the radius vector which constitutes—together with the angular frequency of the planet's rotation $\boldsymbol{\Omega}$—the centrifugal force $\rho\, \boldsymbol{\Omega} \times (\boldsymbol{\Omega} \times \mathbf{x})$, $2\rho\, \boldsymbol{\Omega} \times \mathbf{v}$ is the Coriolis force and the last body force is supplied by the gravitational acceleration $\mathbf{g}$.

If we assume for the constitutive relations that:

$$\mathbb{T} = -p^{\text{th}} \mathbb{I} + \mathbb{S}, \ \lim_{\mathbf{v} \to \mathbf{0}} \mathbb{S} = \mathbf{0}, \tag{3.2}$$

than considering the momentum equation (3.1) in the reference state, we obtain the relation between the reference variables:

$$\nabla p_0^{\text{th}} = \rho_0 \mathbf{g}_0 - \rho_0\, \boldsymbol{\Omega} \times (\boldsymbol{\Omega} \times \mathbf{x}). \tag{3.3}$$

Next, if we ignore variations of the density due to pressure deviations, we can linearise the state equation with respect to the temperature difference $\theta - \theta_0$ to get:

$$\rho = \rho_0 \left(1 - \alpha_{\text{V}} (\theta - \theta_0)\right). \tag{3.4}$$

In numerical modelling of thermal convection it is convenient to define the reference temperature distribution θ_0 as the solution of the following stationary conduction problem:

$$\operatorname{div} (k \nabla \theta_0) + \rho_0 b_e = 0,$$

with boundary conditions given in the problem description (see Figure 3.1). The reader can find more about mathematical modelling of thermal convection in Earth's mantle in lecture notes [Matyska, 2005].

Putting state equation (3.4) into the general form of the continuity equation (1.5) and neglecting the thermal expansion, it follows that for the time-independent variable ρ_0 we have:

$$\operatorname{div} (\rho_0 \mathbf{v}) = 0. \tag{3.5}$$

[i] Joseph Valentin **Boussinesq** (1842–1929) - French mathematician and physicist, known also for approximations of water waves and turbulence

In order to get the approximation of the momentum balance, we plug (3.2)–(3.4) into the specific form of momentum equations (3.1), thus we have:

$$\rho\frac{\mathrm{D}\mathbf{v}}{\mathrm{D}t} = -\nabla\pi + \operatorname{div}\mathbb{S} + \rho_0\beta_{\mathrm{V}}(\theta-\theta_0)\,\boldsymbol{\Omega}\times(\boldsymbol{\Omega}\times\mathbf{x}) - 2\rho\,\boldsymbol{\Omega}\times\mathbf{v} + \\ + \rho_0(\mathbf{g}-\mathbf{g}_0) - \rho_0\beta_{\mathrm{V}}(\theta-\theta_0)(\mathbf{g}-\mathbf{g}_0) - \rho_0\beta_{\mathrm{V}}(\theta-\theta_0)\mathbf{g}_0,$$

where with $\pi = p^{\mathrm{th}} - p_0^{\mathrm{th}}$ we denoted the pressure deviation. Final step towards the linear approximation is to neglect both Corriolis and centrifugal force, along with the quadratic term $\rho_0\beta_{\mathrm{V}}(\theta-\theta_0)(\mathbf{g}-\mathbf{g}_0)$ and the thermal expansion on the right hand side. Thus, we end up with:

$$\rho_0\frac{\mathrm{D}\mathbf{v}}{\mathrm{D}t} = -\nabla\pi + \operatorname{div}\mathbb{S} + \rho_0(\mathbf{g}-\mathbf{g}_0) - \rho_0\beta_{\mathrm{V}}(\theta-\theta_0)\mathbf{g}_0. \tag{3.6}$$

To linearise the temperature conservation of energy, we replace ρ by ρ_0 in the temperature equation (1.45), i.e.:

$$\rho_0 c_p\frac{\mathrm{D}\theta}{\mathrm{D}t} = \mathbb{S}:\mathbb{D} - \operatorname{div}\mathbf{q} + \rho_0 b_e + \alpha_{\mathrm{V}}\theta\frac{\mathrm{D}p^{\mathrm{th}}}{\mathrm{D}t},$$

moreover, we assume that the dominant part of the pressure p^{th} is the hydrostatic pressure, which gives $\mathrm{D}p^{\mathrm{th}}/\mathrm{D}t = -v_{\mathrm{r}}\rho g$, with v_{r} being the radial component of velocity and $g \coloneqq |\mathbf{g}|$ the magnitude of the gravitational acceleration. Assuming referential values (we set $g_0 \coloneqq |\mathbf{g}_0|$) for an isotropic thermally conducting material we obtain the linear approximation of the temperature equation:

$$\rho_0 c_p\frac{\mathrm{D}\theta}{\mathrm{D}t} = \mathbb{S}:\mathbb{D} - \operatorname{div}(k\nabla\theta) + \rho_0 b_e - \rho_0\alpha_{\mathrm{V}}v_{\mathrm{r}}g_0\theta. \tag{3.7}$$

The term $-\rho_0\alpha_{\mathrm{V}}v_{\mathrm{r}}g_0\theta$ is sometimes called the adiabatic heating, since it contains the heat that is produced by compression/expansion due to the vertical movement of the element.

Equations (3.5)–(3.7) constitute the so called *compressible extended (Oberbeck-)Boussinesq approximation*, which we, for the sake of clarity, present once more:

Extended Boussinesq approximation of continuity equation:

$$\operatorname{div}(\rho_0\mathbf{v}) = 0, \qquad \text{in } \omega,$$

Extended Boussinesq approximation of momentum equations:

$$\rho_0\frac{\mathrm{D}\mathbf{v}}{\mathrm{D}t} = -\nabla\pi + \operatorname{div}\mathbb{S} + \rho_0(\mathbf{g}-\mathbf{g}_0) - \rho_0\beta_{\mathrm{V}}(\theta-\theta_0)\mathbf{g}_0, \quad \text{in } \omega,$$

Extended Boussinesq approximation of temperature equation:

$$\rho_0 c_p\frac{\mathrm{D}\theta}{\mathrm{D}t} = \mathbb{S}:\mathbb{D} - \operatorname{div}(k\nabla\theta) + \rho_0 b_e - \rho_0\alpha_{\mathrm{V}}v_{\mathrm{r}}\theta g_0, \qquad \text{in } \omega.$$

To further simplify the previous system of PDEs, we consider the Newtonian fluid, which means $\mathbb{S} = 2\mu\mathbb{D}$, with constant dynamic viscosity μ and apply the system to a problem, where both the referential values ρ_0, $\mathbf{g}_0$ and the

material parameters β_{V}, c_p and k are constant. Finally, if we also omit dissipation $\mathbb{S} : \mathbb{D}$ and the adiabatic heating $-\rho_0 \alpha_{\mathrm{V}} v_{\mathrm{r}} g_0 \theta$, we arrive at the *classical (Oberbeck-)Boussinesq approximation*:

Classical Boussinesq approximation of continuity equation:

$$\operatorname{div} \mathbf{v} = 0, \qquad \text{in } \omega, \tag{3.8}$$

Classical Boussinesq approximation of momentum equations:

$$\rho_0 \frac{\mathrm{D}\mathbf{v}}{\mathrm{D}t} = -\nabla \pi + \mu \Delta \mathbf{v} - \rho_0 \beta_{\mathrm{V}} (\theta - \theta_0) \mathbf{g}_0, \quad \text{in } \omega, \tag{3.9}$$

Classical Boussinesq approximation of temperature equation:

$$\rho_0 c_p \frac{\mathrm{D}\theta}{\mathrm{D}t} = k \Delta \theta + \rho_0 b_e, \qquad \text{in } \omega. \tag{3.10}$$

Nondimensional variables

In the following we will identify ρ with ρ_0 and $\mathbf{g}$ with $\mathbf{g}_0$, neglecting thus the self-gravitation and admitting compressibility only in the buoyancy force $\rho \beta_{\mathrm{V}} (\theta - \theta_0) \mathbf{g}$. There are more possible ways of defining characteristic scales of the system (3.8)–(3.10) depending on what pair of thermomechanical processes we deem most important.

Let us write the following scales of physical variables:

$$\mathbf{x} = \widetilde{\mathbf{x}}\,[\mathbf{x}],\ t = \tilde{t}\,[t],\ \mathbf{v} = \widetilde{\mathbf{v}}\,[\mathbf{v}],\ \theta = \theta_{\mathrm{top}} + \widetilde{\theta}\,[\theta].$$

Primarly, we would like to have a consistent scaling of the velocity and time, i.e.: $[\mathbf{v}] = [\mathbf{x}]/[t]$. This enables the substantial derivative to scale accordingly. Then we can use either of the three following scale factors:

(a) We compare the inertial force and the dissipative viscous term, meaning:

$$\rho \frac{\partial \mathbf{v}}{\partial t} \sim \mu \Delta \mathbf{v},$$
$$\rho \frac{[\mathbf{v}]}{[t]} \frac{\partial \widetilde{\mathbf{v}}}{\partial \tilde{t}} \sim \mu \frac{[\mathbf{v}]}{[\mathbf{x}]^2} \Delta_{\tilde{\mathbf{x}}} \widetilde{\mathbf{v}},$$

where $\Delta_{\tilde{\mathbf{x}}}$ denotes the Laplace operator with respect to nondimensional spatial coordinates. This is a typical scaling for Navier-Stokes equations, for time scale we therefore have:

$$[t] = \frac{\rho}{\mu} [\mathbf{x}]^2 = \frac{[\mathbf{x}]^2}{\nu},$$

with $\nu = \mu/\rho$ the kinematic viscosity, for the velocity scale we get:

$$[\mathbf{v}] = \frac{\nu}{[\mathbf{x}]}.$$

(b) In the second approach, the inertial and the buoyancy force are assumed to be of equal importance, so:

$$\rho \frac{[\mathbf{v}]}{[t]} \frac{\partial \widetilde{\mathbf{v}}}{\partial \tilde{t}} \sim \rho \beta_{\mathrm{V}} g [\theta] (\widetilde{\theta} - \widetilde{\theta}_0) \mathbf{e}_{\hat{z}},$$

where $\mathbf{e}_{\hat{z}}$ is the unit basis vector in the direction of z-axis. This gives:

$$[t] = \sqrt{\frac{[\mathbf{x}]}{\beta_{\mathrm{V}} g[\theta]}} = \frac{[\mathbf{x}]^2}{\nu}\sqrt{\frac{\mathrm{Pr}}{\mathrm{Ra}}},$$

or equivalently for the velocity scale factor:

$$[\mathbf{v}] = \sqrt{\beta_{\mathrm{V}} g[\theta][\mathbf{x}]} = \frac{\nu}{[\mathbf{x}]}\sqrt{\frac{\mathrm{Ra}}{\mathrm{Pr}}}.$$

For convenience, we defined two characteristic numbers:

$$\begin{aligned} &\textit{Rayleigh number:} \quad \mathrm{Ra} = \frac{\beta_{\mathrm{V}} g[\mathbf{x}]^3[\theta]}{\nu\alpha}, \\ &\textit{Prandtl number:} \quad \mathrm{Pr} = \frac{\nu}{\alpha}. \end{aligned}$$

(c) The last possibility is based on similarity of temperature convection and the heat flux, that is:

$$\rho c_p \frac{[\theta]}{[t]}\frac{\partial\widetilde{\theta}}{\partial\widetilde{t}} \sim k\frac{[\theta]}{[\mathbf{x}]^2}\,\Delta_{\tilde{\mathbf{x}}}\,\widetilde{\theta},$$

which gives diffusive time scale:

$$[t] = \frac{[\mathbf{x}]^2}{\alpha} = \frac{[\mathbf{x}]^2}{\nu}\,\mathrm{Pr} \tag{3.11}$$

and respective velocity scale:

$$[\mathbf{v}] = \frac{\alpha}{[\mathbf{x}]}. \tag{3.12}$$

For our non-dimensional formulation scaling (c) is the preffered one. Using (3.11) and (3.12) we modify the momentum equation (3.9) to obtain:

$$\begin{aligned} \frac{1}{\mathrm{Pr}}\rho\frac{\alpha\nu}{[\mathbf{x}]^3}\frac{\mathrm{D}\widetilde{\mathbf{v}}}{\mathrm{D}\widetilde{t}} &= -\nabla\pi + \mu\frac{\alpha}{[\mathbf{x}]^3}\,\Delta_{\tilde{\mathbf{x}}}\,\widetilde{\mathbf{v}} - \rho\beta_{\mathrm{V}} g[\theta](\widetilde{\theta}-\widetilde{\theta}_0)\mathbf{e}_{\hat{z}}, \\ \frac{1}{\mathrm{Pr}}\frac{\mathrm{D}\widetilde{\mathbf{v}}}{\mathrm{D}\widetilde{t}} &= -\nabla_{\tilde{\mathbf{x}}}\,\widetilde{\pi} + \Delta_{\tilde{\mathbf{x}}}\,\widetilde{\mathbf{v}} - \mathrm{Ra}(\widetilde{\theta}-\widetilde{\theta}_0)\mathbf{e}_{\hat{z}}, \end{aligned}$$

with nondimensional pressure difference $\widetilde{\pi} \coloneqq \pi[\mathbf{x}]^2/(\alpha\mu)$. We repeat the idea for the approximation of the temperature equation (3.10). For simplicity we assume $b_e \equiv 0$.

$$\begin{aligned} \rho c_p \frac{[\theta]}{[t]}\frac{\mathrm{D}\widetilde{\theta}}{\mathrm{D}\widetilde{t}} &= k\frac{[\theta]}{[\mathbf{x}]^2}\,\Delta_{\tilde{\mathbf{x}}}\,\widetilde{\theta}, \\ \frac{\mathrm{D}\widetilde{\theta}}{\mathrm{D}\widetilde{t}} &= \Delta_{\tilde{\mathbf{x}}}\,\widetilde{\theta}. \end{aligned}$$

Now we are ready to present the classical formulation of the Blankenbach benchmark problem for two-dimensional thermal convection of the incompressible non-rotating Boussinesq fluid of infinite Prandtl number[ii] (tildes were dropped):

Nondimensional continuity equation:

$$\operatorname{div} \mathbf{v} = 0, \qquad \text{in } \omega, \tag{3.13}$$

Nondimensional momentum equations:[iii]

$$\mathbf{0} = -\nabla\pi + \Delta\mathbf{v} + \mathrm{Ra}(\theta - \theta_0)\mathbf{e}_{\hat{z}}, \quad \text{in } \omega, \tag{3.14}$$

Nondimensional temperature equation:

$$\frac{\mathrm{D}\theta}{\mathrm{D}t} = \Delta\theta, \qquad \text{in } \omega. \tag{3.15}$$

3.1.3 Weak formulation

Again, Rothe method was utilised to solve the problem numerically, which means that we need to define the variational problem at each time step. First, let us define the following function spaces:

$$\begin{aligned}
\mathcal{P} &\coloneqq \{\varpi \in L^2(\omega) \mid \int_\omega \varpi \,\mathrm{d}\mathbf{x} = 0\},\\
\mathcal{V} &\coloneqq H^1(\omega),\\
\mathcal{T} &\coloneqq \{\vartheta \in H^1(\omega) \mid \vartheta|_{\gamma_\mathrm{t}\cup\gamma_\mathrm{b}} = 0\}.
\end{aligned}$$

Also, let $\Theta_\mathrm{D} \in H^1(\omega)$ be the representative of the Dirichlet boundary conditions for temperature, then the weak formulation follows.

At $t = t^k$ we look for $(\pi, \mathbf{v}, \theta - \Theta_\mathrm{D}) \in \mathcal{P} \times \mathcal{V} \times \mathcal{T}$, such that:

$$\begin{aligned}
0 &= \int_\omega (\operatorname{div}\mathbf{v})\varpi \,\mathrm{d}\mathbf{x},\\
0 &= \int_\omega \pi \operatorname{div}\mathbf{u} - \nabla\mathbf{v} : \nabla\mathbf{u} + \mathrm{Ra}(\theta - \theta_0)\mathbf{e}_{\hat{z}} \cdot \mathbf{u} \,\mathrm{d}\mathbf{x},\\
\int_\omega \frac{\theta}{\Delta t}\vartheta \,\mathrm{d}\mathbf{x} &= \int_\omega \nabla\theta \cdot \nabla\vartheta - (\mathbf{v}\cdot\nabla\theta)\vartheta + \frac{\theta^{k-1}}{\Delta t}\vartheta \,\mathrm{d}\mathbf{x}, \ \forall(\varpi, \mathbf{u}, \vartheta) \in \mathcal{P}\times\mathcal{V}\times\mathcal{T}.
\end{aligned}$$

3.2 Free surface

We are now going to make one step further and introduce the free surface into the formulation of our problem. As was mentioned in the beginning of the chapter, this obstacle will be attacked using ALE formulation, whose essentials are addressed in subsection 3.2.2.

[ii] Values from Table 1 of [Blankenbach et al., 1989] give $1/\mathrm{Pr} = 4 \cdot 10^{-26}$.

[iii] Equivalently, we can formulate momentum equations for nondimensional pressure p^th, instead of pressure deviation π. This would give following set of equations:

$$\mathbf{0} = -\nabla p^\mathrm{th} + \Delta\mathbf{v} + \mathrm{Ra}(\theta - \theta_0)\mathbf{e}_{\hat{z}} + \frac{\mathrm{Ra}}{\beta_\mathrm{V}[\theta]}\mathbf{e}_{\hat{z}}.$$

3.2.1 Problem formulation

Free surface dynamical boundary condition $\mathbb{S}\mathbf{n}|_{\gamma_t} = \mathbf{0}$ and variable cell height $h(x)$ are the only differences in the free surface Blankenbach benchmark problem formulation. The formulation is, again, graphically summarised in Figure 3.2. A kinematical boundary condition for the free surface γ_t is discussed later.

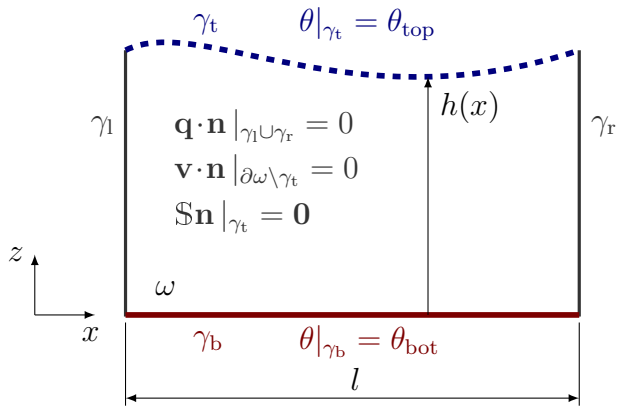

Figure 3.2: Formulation of the Blankenbach benchmark with free surface.

3.2.2 ALE formulation

Method description

There are two main possible kinematical descriptions of continuum, that fundamentally influence a formulation and numerical solution of a physical problem.

The first one is called *Lagrangian* and it is preferred in structural mechanics. With this approach free surfaces and interfaces between subdomains are easily trackable on one hand, but on the other hand large distorsions may lead to a complete breakdown of a computational mesh. The cause of this effect lies in the fact that using Lagrangian description one tracks the same material point $\mathbf{X}$ whose position is given with respect to some referential (here material) configuration Ω at time t_0.

Existence of such a referential configuration is crucial in the first approach and it is not always guaranteed (as is the case of fluids). *Eulerian description* is able to remedy such situations, since the computational mesh is fixed and the spatial points $\mathbf{x}$ from current configuration ω are those we work with. Grid configuration can cope with possibly large distorsions of the continuum at the expense of loss of information about precise interface position. A connection between the material and the current configuration is provided by the mapping

$$\boldsymbol{\chi} : [t_0, T) \times \Omega \to [t_0, T) \times \omega;\ (t, \mathbf{X}) \mapsto \boldsymbol{\chi}(t, \mathbf{X}) = (t, \mathbf{x}).$$

Arbitrary Lagrangian-Eulerian description was developped with the intension to combine the best features of the previous approaches and can be viewed as a generalisation of both of them. It makes use of a third configuration $\omega_{\boldsymbol{\xi}}$ whose elements are identified with the computational grid points. Mappings

$$\boldsymbol{\Psi} : [t_0, T) \times \omega_{\boldsymbol{\xi}} \to [t_0, T) \times \Omega;\ (t, \boldsymbol{\xi}) \mapsto \boldsymbol{\Psi}(t, \boldsymbol{\xi}) = (t, \mathbf{X}),$$
$$\boldsymbol{\varphi} : [t_0, T) \times \omega_{\boldsymbol{\xi}} \to [t_0, T) \times \omega;\ (t, \boldsymbol{\xi}) \mapsto \boldsymbol{\varphi}(t, \boldsymbol{\xi}) = (t, \mathbf{x})$$

provide relationship to the material, respectively current configuration. Although the choice of the reference configuration $\omega_{\boldsymbol{\xi}}$ is arbitrary, the mappings are linked through the following relation:

$$\boldsymbol{\chi} = \boldsymbol{\varphi} \circ \boldsymbol{\Psi}^{-1}. \tag{3.16}$$

It is physically reasonable to assume the mapping $\boldsymbol{\chi}$ to be one-to-one, meaning $\det(\partial\boldsymbol{\chi}/\partial\mathbf{X}) > 0$ everywhere. This, by the previous relation, justifies the existence of $\boldsymbol{\Psi}^{-1}$. Special choice of mapping $\boldsymbol{\varphi}$ or $\boldsymbol{\Psi}$ might give us back either Lagrangian ($\boldsymbol{\Psi}^{-1} \equiv \mathrm{id}_\Omega$) respectively Eulerian ($\boldsymbol{\varphi}^{-1} \equiv \mathrm{id}_\omega$) description. Figure 3.3 shows an attempt to capture these relations graphically. The possibility of an arbitrary mesh deformation comes with a drawback in the form of a necessity of the correct definition of the grid velocities as well as a supply of an automated mesh-update algorithm.

Applications of the ALE method in both the fluid and the solid mechanics are presented in [Donea et al., 2004]. The same reference contains a survey of mesh update and mesh adaptation procedures. [Scovazzi and J. R. Hughes, 2007] covers the theory of ALE formulation and contains derivation of conservation principles in the ALE description of motion.

Every kinematical description, specified by a particular mapping, induce a respective velocity, given by a time derivative of the mapping. Thus we introduce

$$\mathbf{v}(t,\mathbf{x}) \coloneqq \frac{\partial\boldsymbol{\chi}}{\partial t}(t,\mathbf{X}), \hat{\mathbf{v}}(t,\boldsymbol{\xi}) \coloneqq \frac{\partial\boldsymbol{\varphi}}{\partial t}(t,\boldsymbol{\xi}), \mathbf{w}(t,\mathbf{X}) \coloneqq \frac{\partial\boldsymbol{\Psi}^{-1}}{\partial t}(t,\mathbf{X}),$$

to be the material velocity of a particle $\mathbf{X}$, respectively mesh velocity of a mesh node $\boldsymbol{\xi}$ and the particle velocity of $\mathbf{X}$ in the reference domain $\omega_{\boldsymbol{\xi}}$. From (3.16) we see that:

$$\mathbf{v}(t,\mathbf{x}) = \frac{\partial}{\partial t}\boldsymbol{\varphi}(t,\boldsymbol{\Psi}^{-1}(t,\mathbf{X}))|_{\mathbf{x}} = \hat{\mathbf{v}}(t,\mathbf{x}) + \frac{\partial\mathbf{x}}{\partial\boldsymbol{\xi}}\mathbf{w}(t,\mathbf{X})|_{\mathbf{x}},$$

where $|_{\mathbf{x}}$ means that we keep $\mathbf{x}$ fixed. So we can define the convective velocity $\mathbf{c}$, which expresses the relative velocity between the mesh and the material, by the following:

$$\mathbf{c} \coloneqq \mathbf{v} - \hat{\mathbf{v}} = \frac{\partial\mathbf{x}}{\partial\boldsymbol{\xi}}\mathbf{w}. \tag{3.17}$$

Now we would like to express the material derivative of a scalar function f with respect to the computational grid represented by the coordinates $\boldsymbol{\xi}$, which, again, calls for an application of the chain rule:

$$\begin{aligned}\frac{\partial}{\partial t} f\left(t, \boldsymbol{\Psi}^{-1}(t,\mathbf{X})\right)\Big|_{\mathbf{X}} = \left.\frac{\partial f}{\partial t}\right|_{\boldsymbol{\xi}} + \frac{\partial f}{\partial\boldsymbol{\xi}}\cdot\mathbf{w} = \left.\frac{\partial f}{\partial t}\right|_{\boldsymbol{\xi}} + \left(\frac{\partial\mathbf{x}}{\partial\boldsymbol{\xi}}\right)^T\frac{\partial f}{\partial\mathbf{x}}\cdot\mathbf{w} = \\ \overset{(3.17)}{=} \left.\frac{\partial f}{\partial t}\right|_{\boldsymbol{\xi}} + \nabla f\cdot\mathbf{c}.\end{aligned} \tag{3.18}$$

Using the expression (3.18) for the material derivative corresponding to grid node $\boldsymbol{\xi}$ we can rearrange the differential form of mass balance (1.4), momentum

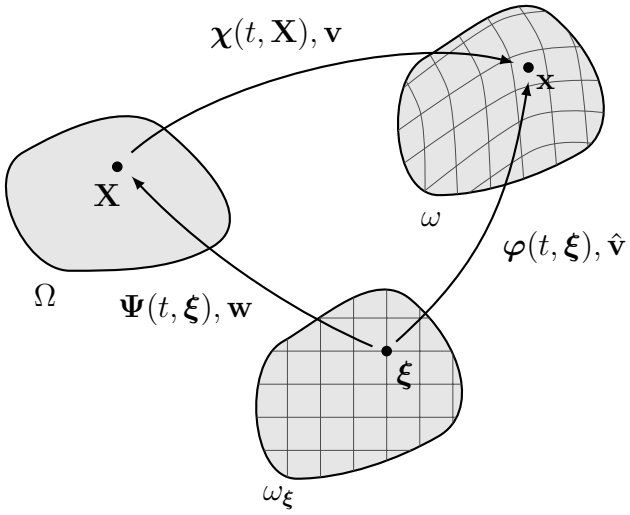

(a) Arbitrary Lagrangian-Eulerian description.

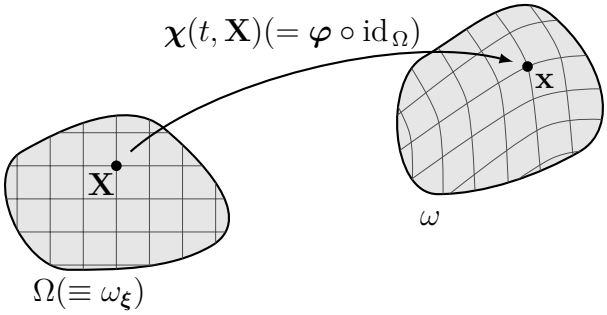

(b) Lagrangian kinematic description.

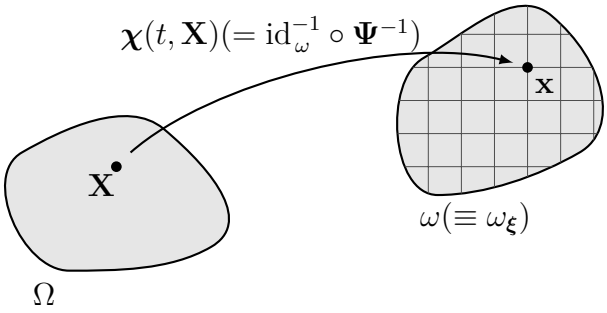

(c) Eulerian kinematic description.

Figure 3.3: Illustration of various kinematic descriptions commonly used in continuum mechanics.

equations (1.8) and the internal energy conservation (1.21) simply by substituting

c for the convective velocity on the left hand side:

ALE form of continuity equation:

$$\left.\frac{\partial \rho}{\partial t}\right|_{\boldsymbol{\xi}} + \mathbf{c} \cdot \nabla \rho = -\rho \operatorname{div} \mathbf{v} \qquad \text{in } \omega(t), \tag{3.19}$$

ALE form of momentum equations:

$$\rho \left(\left.\frac{\partial \mathbf{v}}{\partial t}\right|_{\boldsymbol{\xi}} + (\nabla \mathbf{v})\mathbf{c} \right) = \operatorname{div} \mathbb{T} + \rho \mathbf{b} \qquad \text{in } \omega(t), \tag{3.20}$$

ALE form of energy equation:

$$\rho \left(\left.\frac{\partial e}{\partial t}\right|_{\boldsymbol{\xi}} + \mathbf{c} \cdot \nabla e \right) = \mathbb{T} : \mathbb{D} - \operatorname{div} \mathbf{q} + \rho b_e \quad \text{in } \omega(t). \tag{3.21}$$

Weak formulation and Nitsche's method

There are two possible ways how to compute the unknown position of the free surface γ_{t}. A more general approach is simply to impose $\mathbf{w} \cdot \mathbf{n} = 0$ on γ_{t} meaning that no particle can cross the free surface. The second approach give us the position of the surface directly. We assume $\varphi(t, \boldsymbol{\xi})$ to denote the vertical displacement of the node $\boldsymbol{\xi} = (\xi^x, \xi^z)$ at the time t and for the spatial point $\mathbf{x}_{\mathrm{t}}(t) = (x_{\mathrm{t}}(t), z_{\mathrm{t}}(t))$ on the top boundary $\gamma_{\mathrm{t}}(t)$ we can write:

$$\begin{aligned} x_{\mathrm{t}}(t) &= \xi^x_{\mathrm{t}} = \xi^x, \\ z_{\mathrm{t}}(t) &= \varphi(t, \xi^x_{\mathrm{t}}, \xi^z_{\mathrm{t}}) = \varphi(t, x_{\mathrm{t}}, \xi^z_{\mathrm{t}}). \end{aligned}$$

Thus we can introduce a new (Eulerian) variable

$$h(t, x) \coloneqq \varphi(t, x, \xi^z)|_{\xi^z = \xi^z_{\mathrm{t}}},$$

which immediately gives:

$$z_{\mathrm{t}}(t) = h(t, x_{\mathrm{t}}).$$

Taking a time derivative of this equation we obtain the kinematic equation for γ_{t}:

$$\frac{\partial h}{\partial t} + \frac{\partial h}{\partial x} v_x = v_z. \tag{3.22}$$

Continuous rezoning of the mesh is provided by the so called *Laplacian smoothing*, which is able to form lines of equal potential for convex, logically regular domains. We look for a mapping φ that is a harmonic extension of h on the whole domain. Thus, we have that $\varphi|_{\gamma_{\mathrm{t}}} = h$ and we can rewrite the kinematic equation for γ_{t} (3.22) in terms of φ:

$$\frac{\partial \varphi}{\partial t} + \frac{\partial \varphi}{\partial x} v_x = v_z, \text{ on } \gamma_{\mathrm{t}}(t).$$

Then, we apply the temporal discretisation and recast the kinematic equation in the following form:

$$\varphi - \varphi^{k-1} + \Delta t \left(\frac{\partial \varphi}{\partial x} v_x - v_z \right) = 0, \quad \text{on } \gamma_{\mathrm{t}}(t^{k-1}), \tag{3.23}$$

All in all, we solve the following problem for the time $t = t^{k+1}$:

$$\begin{aligned} -\Delta\varphi = -\frac{\partial^2\varphi}{\partial x^2} - \frac{\partial^2\varphi}{\partial z^2} = 0 \quad & \text{in } \omega(t^k), \\ \varphi - \varphi^{k-1} + \Delta t \left(\frac{\partial\varphi}{\partial x} v_x - v_z \right) = 0 \quad & \text{on } \gamma_{\mathrm{t}}(t^k), \\ \frac{\partial\varphi}{\partial x} = 0 \quad & \text{on } \gamma_{\mathrm{l}} \cup \gamma_{\mathrm{r}}(t^{k-1}), \\ \varphi = 0 \quad & \text{on } \gamma_{\mathrm{b}}. \end{aligned}$$

Solution of the problem gives us the mesh displacement mapping at the time $t = t^k$, that is $\boldsymbol{\varphi}(t^k, \cdot) =: \boldsymbol{\varphi}_k = (0, \varphi)$. This application of ALE method is sometimes called *incremental (or poorman's) ALE method*.

Using a generalisation of the *Nitsche's method* described in [Juntunen and Stenberg, 2009], we can incorporate the boundary condition into the weak formulation. Let us apply this approach to our problem. A specific form of the boundary condition is considered in the article, namely:

$$\frac{\partial\varphi}{\partial n} = \frac{1}{\epsilon}(\varphi_0 - \varphi) + g \quad \text{on } \gamma_{\mathrm{t}}(t^{k-1}), \tag{3.24}$$

where $\partial\varphi/\partial n \coloneqq \nabla\varphi \cdot \mathbf{n}$ denotes the normal derivative and $\epsilon \in [0, \infty]$ is a parameter, whose limiting values give either the Dirichlet or the Neumann boudnary condition. The weak formulation of the Laplace problem using Nitsche's method is represented by equations (2.4)–(2.6) in [Juntunen and Stenberg, 2009], where the right hand side $f \equiv 0$, that is:

At the time $t = t^k$ we look for $\varphi \in H^1(\omega(t^{k-1}))$, such that:

$$\begin{aligned} \int_{\omega(t^{k-1})} \nabla\varphi \cdot \nabla\phi \,\mathrm{d}\mathbf{x} + \sum_{E \in \mathcal{G}_h(t^{k-1})} \Bigg(& -\frac{\gamma h_E}{\epsilon + \gamma h_E} \int_E \frac{\partial\varphi}{\partial n}\phi + \varphi\frac{\partial\phi}{\partial n} \,\mathrm{d}a + \\ & + \frac{1}{\epsilon + \gamma h_E} \int_E \varphi\phi \,\mathrm{d}a - \frac{\epsilon\gamma h_E}{\epsilon + \gamma h_E} \int_E \frac{\partial\varphi}{\partial n}\frac{\partial\phi}{\partial n} \,\mathrm{d}a \Bigg) = \\ = \sum_{E \in \mathcal{G}_h(t^{k-1})} \Bigg(& \frac{1}{\epsilon + \gamma h_E} \int_E \varphi_0\phi \,\mathrm{d}a + \frac{\gamma h_E}{\epsilon + \gamma h_E} \int_E \varphi_0 \frac{\partial\phi}{\partial n} \,\mathrm{d}a + \\ & + \frac{\epsilon}{\epsilon + \gamma h_E} \int_E g\phi \,\mathrm{d}a - \frac{\epsilon\gamma h_E}{\epsilon + \gamma h_E} \int_E g\frac{\partial\phi}{\partial n} \,\mathrm{d}a \Bigg), \ \forall\phi \in H^1(\omega(t^{k-1})), \end{aligned} \tag{3.25}$$

where by E we denote an edge in the partitioning $\mathcal{G}_h(t^{k-1})$ of the free surface $\gamma_{\mathrm{t}}(t^{k-1})$, h_E is the diameter of the edge E and γ is a parameter whose certain values ensure stability of the modified formulation.

Taking the limit $\epsilon \to 0$ in (3.25), we can obtain the following variational equality:

$$\begin{aligned} \int_{\omega(t^{k-1})} \nabla\varphi \cdot \nabla\phi \,\mathrm{d}\mathbf{x} = \sum_{E \in \mathcal{G}_h(t^{k-1})} \int_E (\varphi_0 - \varphi) \left(\frac{1}{\gamma h_E}\phi - \frac{\partial\phi}{\partial n} \right) + \frac{\partial\varphi}{\partial n}\phi \,\mathrm{d}a, \\ \forall\phi \in H^1(\omega(t^{k-1})). \end{aligned} \tag{3.26}$$

The same limit in (3.24) gives the Dirichlet boundary condtion:

$$\varphi_0 - \varphi = 0 \quad \text{on } \gamma_{\mathrm{t}}(t^{k-1}). \tag{3.27}$$

It remains to realize that the discretised kinematic equation (3.23) does not exactly match (3.27), nevertheless it can be viewed as an implicit form of the Dirchlet boundary condition. The weak formulation (3.26) is transformed into:

$$\int_{\omega(t^{k-1})} \nabla\varphi \cdot \nabla\phi \,\mathrm{d}\mathbf{x} =$$
$$= \sum_{E\in\mathcal{G}_h(t^{k-1})} \int_E \left((\varphi - \varphi^{k-1} + \Delta t \left(\frac{\partial\varphi}{\partial x} v_x - v_z\right)\right)\left(\frac{1}{\gamma h_E}\phi - \frac{\partial\phi}{\partial n}\right) + \frac{\partial\varphi}{\partial n}\phi \,\mathrm{d}a,$$
$$\forall\phi \in H^1(\omega(t^{k-1})).$$

Before we present the final formulation of the free surface problem, we call the reader's attention to the computational inconvenience that is described in [Kaus et al., 2010]. Earth mantle convection codes for free surface problems may experience an instability, that is sometimes called the drunken sailor effect. It is depicted in Figure 3.4. A time step that is small enough to limit the vertical displacement of the free surface can prevent the instabillity from ocurring. But such a restriction on the time discretisation may cause an increase of computational time. We therefore introduce a counteracting boundary traction in the momentum equations, it has the following form:

$$\mathbf{t}^g = -\lambda\Delta t\rho g(\mathbf{v}\cdot\mathbf{n})\mathbf{e}_{\hat{z}},$$

where $\lambda \in [0, 1]$ denotes the weighting parameter of the counteracting force.

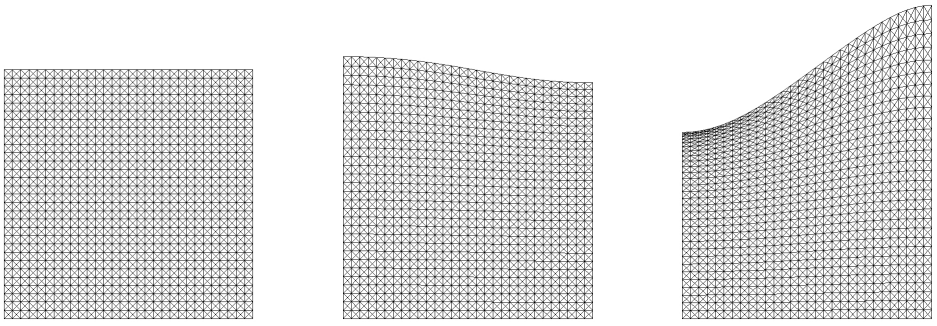

(a) $t = 0\,\mathrm{s}$. (b) $t = 1 \cdot 10^{-5}\,\mathrm{s}$. (c) $t = 2 \cdot 10^{-5}\,\mathrm{s}$.

Figure 3.4: Drunken sailor effect.

FEM formulation

We are ready to present the finite element formulation of the free surface problem in its entirety. First, let us clarify, that we used P1/P2/P2 elements for the thermomechanical problem, i.e. at the time $t = t^k$ we use the following definitions of spaces:

$$\begin{aligned}
\mathcal{P}_h^k &:= \{\pi_h \in C\left(\omega(t^k)\right) \mid \pi_h|_T \in P_1(T), \forall T \in \mathcal{T}_h(t^k)\},\\
\mathcal{V}_h^k &:= \{\mathbf{v}_h \in C\left(\omega(t^k)\right) \mid \mathbf{v}_h|_T \in P_2(T)^2, \forall T \in \mathcal{T}_h(t^k), \mathbf{v}_h|_{\gamma_{\mathrm{t}}(t^k)} = \hat{\mathbf{v}}\},\\
\Theta_h^k &:= \{\theta_h \in C\left(\omega(t^k)\right) \mid \theta_h|_T \in P_2(T), \forall T \in \mathcal{T}_h(t^k), \theta_h|_{\gamma_{\mathrm{b}}} = 1, \theta_h|_{\gamma_{\mathrm{t}}(t^k)} = 0\},
\end{aligned}$$

where $\mathcal{T}_h(t^k)$ represents the triangulation of $\omega(t^k)$. Search space of the mesh displacement problem is approximated by:

$$\Phi_h^k := \{\varphi_h \in C\left(\omega(t^{k-1})\right) \mid \varphi_h|_T \in P_1(T), \forall T \in \mathcal{T}_h(t^{k-1})\}.$$

FEM formulation of the free surface problem at the time $t = t^k$:

Mesh update: $\varphi_h \in \Phi_h^k$:

$$\begin{aligned}
&\int_{\omega(t^{k-1})} \nabla\varphi_h \cdot \nabla\phi_h \,\mathrm{d}\mathbf{x} =\\
&= \sum_{E\in\mathcal{G}_h(t^{k-1})} \int_E \left((\varphi - \varphi^{k-1} + \Delta t\left(\frac{\partial\varphi}{\partial x}v_x - v_z\right)\right)\left(\frac{1}{\gamma h_E}\phi_h - \frac{\partial\phi_h}{\partial n}\right) + \frac{\partial\varphi_h}{\partial n}\phi_h \,\mathrm{d}a,\\
&\qquad\qquad \forall\phi_h \in \Phi_h^k,
\end{aligned}$$

Thermomechanical problem: $(\pi_h, \mathbf{v}_h, \theta_h) \in \mathcal{P}_h^k \times \mathcal{V}_h^k \times \Theta_h^k$:

$$\begin{aligned}
0 &= \int_{\omega(t^k)} (\operatorname{div}\mathbf{v}_h)\varpi_h \,\mathrm{d}\mathbf{x},\\
0 &= \int_{\omega(t^k)} \pi_h \operatorname{div}\mathbf{u}_h - \nabla\mathbf{v}_h : \nabla\mathbf{u}_h + \mathrm{Ra}(\theta_h - \theta_{0,h})\mathbf{e}_{\hat{z}} \cdot \mathbf{u}_h \,\mathrm{d}\mathbf{x} -\\
&\qquad - \int_{\gamma_{\mathrm{t}}(t^k)} \lambda\frac{\mathrm{Ra}}{\beta_{\mathrm{V}}[\theta]}\Delta t(\mathbf{v}_h \cdot \mathbf{n})(e_z \cdot \mathbf{u}_h) \,\mathrm{d}a,\\
\int_{\omega(t^k)} \frac{\theta_h}{\Delta t}\vartheta_h \,\mathrm{d}\mathbf{x} &= \int_{\omega(t^k)} \nabla\theta_h \cdot \nabla\vartheta_h - \left((\mathbf{v}_h - \hat{\mathbf{v}}_h) \cdot \nabla\theta_h\right)\vartheta_h + \frac{\theta_h^{k-1}}{\Delta t}\vartheta_h \,\mathrm{d}\mathbf{x},\\
&\qquad\qquad \forall(\varpi_h, \mathbf{u}_h, \vartheta_h) \in \mathcal{P}_h^k \times \mathcal{V}_h^k \times \Theta_h^k.
\end{aligned}$$

When the solution of the mesh update problem is constructed, we modify the mesh using automated FEniCS algorithm `ALE.move()`. The convective velocity $\mathbf{v}_h - \hat{\mathbf{v}}_h$ in the temperature equation is the relative velocity $\mathbf{c}$ that arises due to the ALE fomrulation of the problem. The velocity of the mesh $\hat{\mathbf{v}}_h$ is computed from the mesh displacement field, i.e.:

$$\hat{\mathbf{v}}_h = \frac{\varphi_h - \varphi_h^{k-1}}{\Delta t}.$$

Parameters with values for both the fixed domain and the free surface problem are tabulated in Table 3.1.

	Parameter	Value
Geometry	l	$10^6\,\mathrm{m}$
	h	$10^6\,\mathrm{m}$
Material quantity	β_V	$2.5 \cdot 10^{-5}\,\mathrm{K}^{-1}$
Scales	$[\mathbf{x}]$	$10^6\,\mathrm{m}$
	$[\theta]$	$\Delta\theta \coloneqq \theta_\mathrm{bot} - \theta_\mathrm{top} = 1000\,\mathrm{K}$
Formulation/discretisation	θ_0	$0\,\mathrm{K}$
	θ_top	$0\,\mathrm{K}$
	θ_bot	$1000\,\mathrm{K}$
	x_div	30
	z_div	30
	Δt [a]	$10^{-4}[\theta] = 10^{14}\,\mathrm{s}$
	Ra	10^4
	γ	0.005
	h_E	$1/x_\mathrm{div}$
	λ	1

Note: [a] This denotes the initial time step, CFL condition was applied after the first cycle of the time loop was completed.

Table 3.1: Numerical values of parameters for Blankenbach benchmark problem.

3.3 Results

3.3.1 Benchmark data

Two nondimensional quantities were collected during the computation:

- *Nusselt number:*

$$\mathrm{Nu} = -h\frac{\int_{\gamma_\mathrm{t}} \partial\theta/\partial z \,\mathrm{d}s}{\int_0^l \theta\,|_{z=0}(x)\,\mathrm{d}x},$$

- *rms velocity:*

$$v_\mathrm{rms} = \frac{h}{\alpha}\sqrt{\frac{1}{hl}\int_0^l\int_0^h |\mathbf{v}|^2\,\mathrm{d}z\,\mathrm{d}x}.$$

Figure 3.5 and Figure 3.6 show that the free surface formulation give consistent benchmark results.

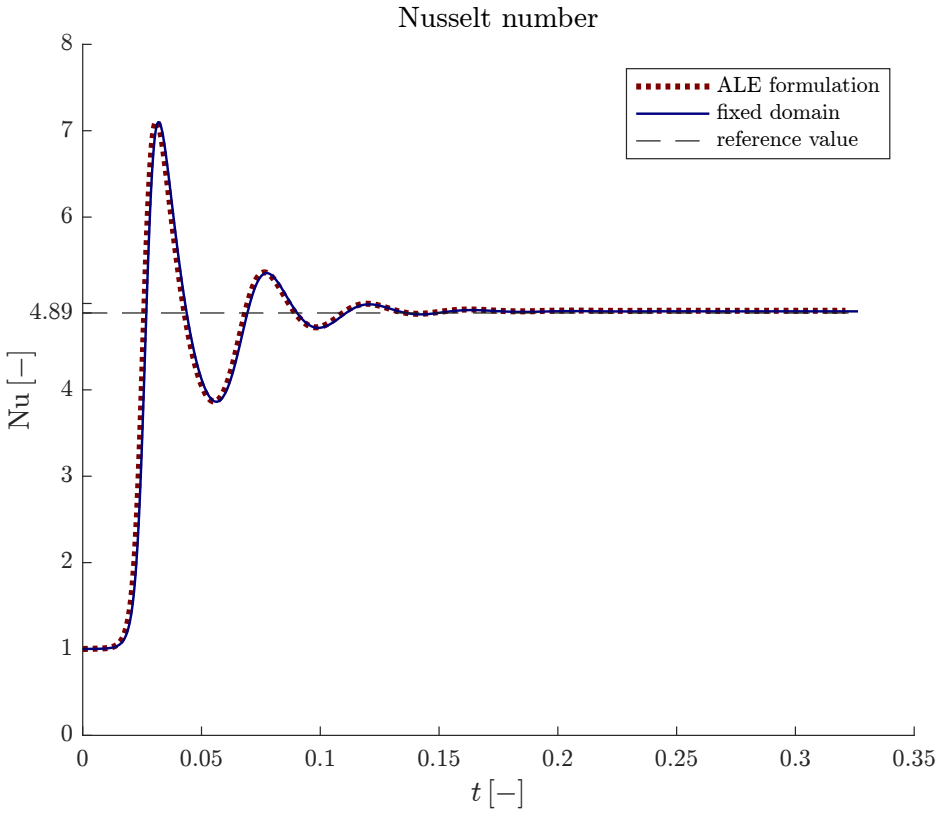

Figure 3.5: Nusselt number data correlation for ALE and fixed domain formulation. The black dashed line denotes the representative value given by the benchmark reference.

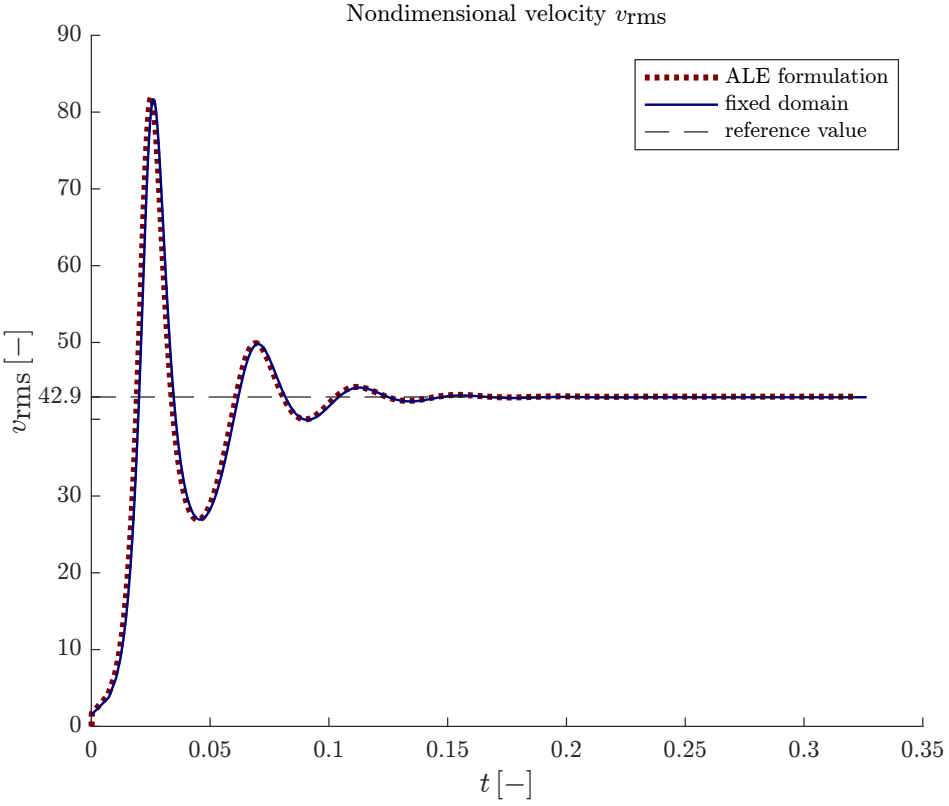

Figure 3.6: Nondimensional velocity v_{rms} data correlation for ALE and fixed domain formulation.

3.3.2 Dynamic topography vs. ALE mesh displacement

We employed the ALE technique to account for the moving upper surface, whose displacement is given as a solution of the Laplacian smoothing mesh-update procedure. Precision of such transformation is difficult to measure. We decided to compare mesh displacement at the upper left corner of the domain with so called dynamic topography, which constitutes approximation of the water surface deflection based simply on a balance of gravitational and surface forces, expressed mathematically:

$$\rho g \Delta h = -\mathbf{n}_{\gamma_{\mathrm{t}}} \cdot \mathbb{T}\mathbf{n}_{\gamma_{\mathrm{t}}} = -T_{zz},$$

where Δh is the upper left corner horizontal deflection (increase with respect to the height of the cell h) and $\mathbf{n}_{\gamma_{\mathrm{t}}}$ denotes the unit outer normal of the upper surface which for the fixed domain equals $\mathbf{e}_{\hat{z}} = (0, 1)$. Since the Cauchy stress tensor is scaled with $[\mathbf{x}]^2/(\alpha\mu)$, we can write for nondimensional deflection:

$$\Delta\widetilde{h} = -\frac{\beta_{\mathrm{V}}\mu}{\rho g[\mathbf{x}]^3}\widetilde{T}_{zz} = -\frac{\beta_{\mathrm{V}}[\theta]}{\mathrm{Ra}}\widetilde{T}_{zz}.$$

To get the variations of the dynamic topography, we need to subtract the average value given by $\int_{\gamma_{\mathrm{t}}} \Delta h \, \mathrm{d}s$. Figure 3.7 gives the resulting comparison in the dimensional form.

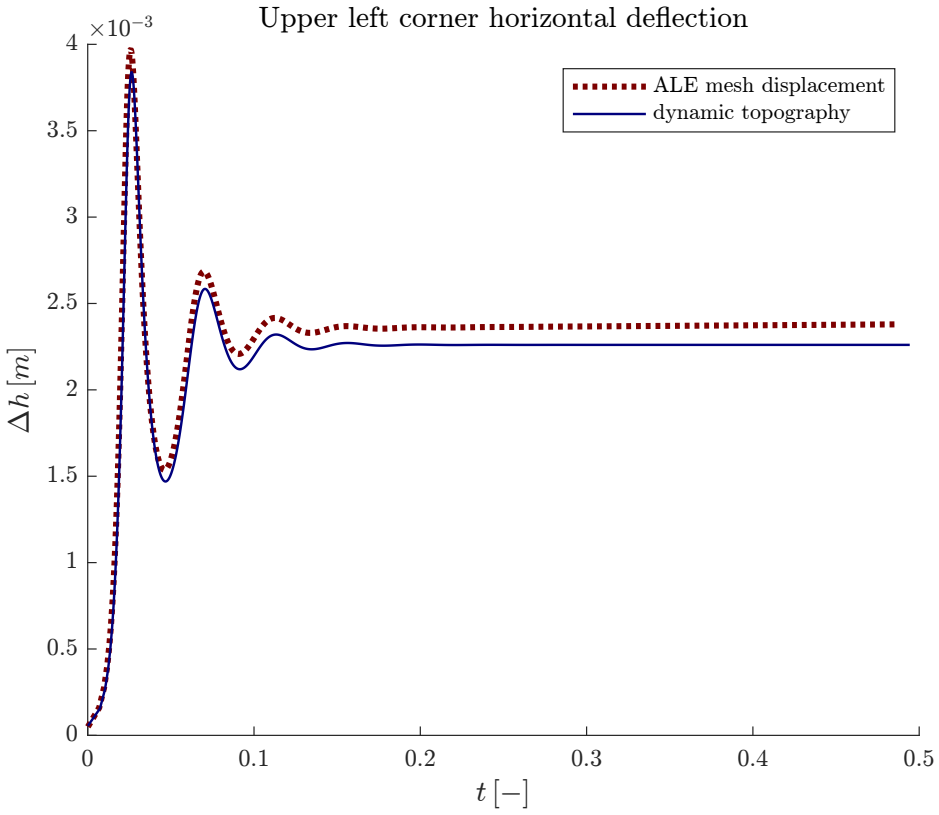

Figure 3.7: Comparison of variations of the left corner horizontal coordinate given by ALE mesh-update procedure and dynamic topography approximation.

Conclusions and perspectives

The thesis proved that the proposed numerical tools are suitable for the problem that is formulated in Chapter 1. Enthalpy method, that was derived from the postulated thermomechanical potential of internal energy, demonstrated to be a very robust tool for phase-change problems. Suprisingly, it presented precise results even for the two dimensional Stefan problem on a coarse mesh. Computational stability of the one-dimensional Stefan problem FEM formulation showed valuable restriction on discretisation parameters of the problem. These restrictions were validated by a computation and the results are depicted in Figure 2.4.

In Chapter 3 we attacked the second problematic aspect of our problem—the free surface. ALE formulation was applied to the problem and the incremental method was presented in the FEM formulation. Results of the Blankenbach benchmark showed good agreement with the data presented in the reference ([Blankenbach et al., 1989]). The upper boundary elevation, given by the dynamic topography approximation, was compared with the solution of the mesh update problem. The results exhibited a relatively small disagreement, which was expected, since the dynamic topography approach provides only a first-order approximation.

Unfortunately, due to lack of time I was unable to complete the simulation of a Stokes problem with the phase transition. The formulation, inspired by [Danaila et al., 2014], is given by the following system:

$$\begin{aligned}
\operatorname{div}\mathbf{v} &= 0,\\
\frac{\mathrm{D}\mathbf{v}}{\mathrm{D}t} &= -\nabla\pi + 2\operatorname{div}(\mu_\epsilon\mathbb{D}) + \frac{\mathrm{Ra}}{\mathrm{Pr}\,\mathrm{Re}^2}\frac{1}{\beta_\mathrm{V}(\theta_\mathrm{h}-\theta_\mathrm{c})}\frac{\rho(\theta)-\rho(\theta_\mathrm{m})}{\rho(\theta_\mathrm{m})},\\
(c_\mathrm{p})_\epsilon\frac{\mathrm{D}\theta}{\mathrm{D}t} &= \frac{1}{\mathrm{Pr}}\operatorname{div}(k_\epsilon\nabla 1\theta),
\end{aligned}$$

where θ_h is the temperatured of the heated (left) wall and θ_c is the temperature of the opposite cold wall. State equation for ρ is given by:

$$\rho(\theta) = \rho_\mathrm{m}\left(1 - w\left|\theta-\theta_\mathrm{m}\right|^q\right),$$

with $\rho_\mathrm{m} = 999.972\,\mathrm{kg/m^3}$, $w = 9.2793\cdot 10^{-6}\,(^\circ\mathrm{C})^{-q}$ and $q = 1.894816$.

Some preliminary results were obtained, but further investigation will be a topic of the disertation.

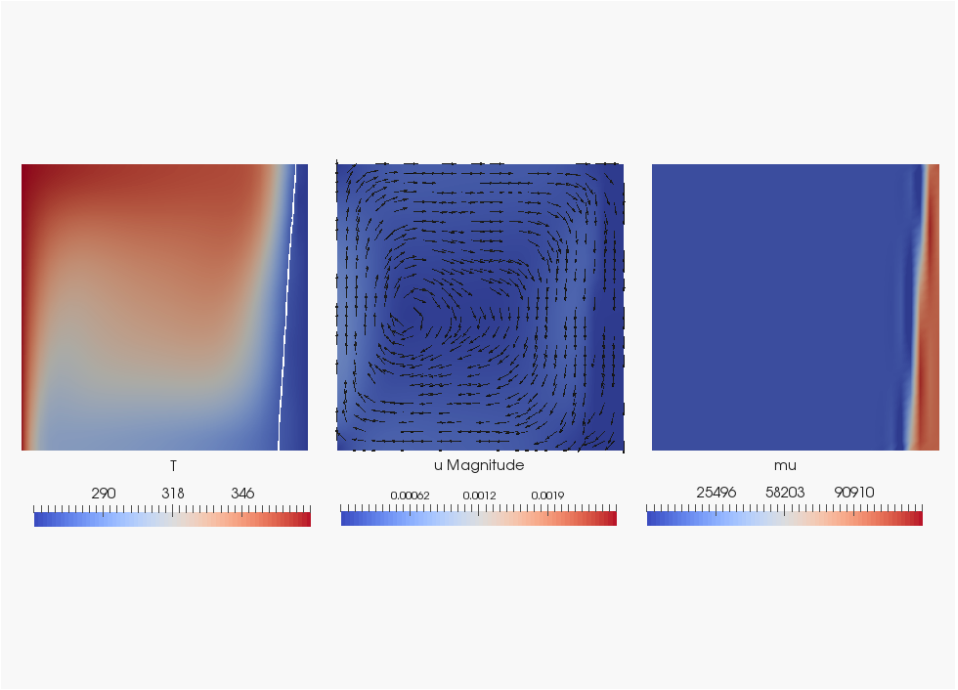
T
290
318
346
u Magnitude
0.00062
0.0012
0.0019
mu
25496
58203
90910

Bibliography

Vasilios Alexiades and Alan D. Solomon. *Mathematical Modeling of Melting and Freezing Processes*. Hemisphere Pub. Corp., 1993. ISBN 1-56032-125-3.

Mikael Beuthe. Enceladus's Crust as a Non-uniform Thin Shell: I Tidal Deformations. *Icarus*, 302:145–174, 2018. doi: 10.1016/j.icarus.2017.11.009.

B. Blankenbach, F. Busse, U. Christensen, L. Cserepes, D. Gunkel, U. Hansen, H. Harder, G. Jarvis, M. Koch, G. Marquart, and et al. A benchmark comparison for mantle convection codes. *Geophysical Journal International*, 98(1): 23–38, 1989. doi: 10.1111/j.1365-246x.1989.tb05511.x.

Ionut Danaila, Raluca Moglan, Frédéric Hecht, and Stéphane Le Masson. A newton method with adaptive finite elements for solving phase-change problems with natural convection. *Journal of Computational Physics*, 274:826–840, 2014. doi: 10.1016/j.jcp.2014.06.036.

Jean Donea, Antonio Huerta, Jean-Philippe Ponthot, and Antonio Rodríguez-Ferran. Arbitrary lagrangian-eulerian methods. *Encyclopedia of Computational Mechanics*, page 1–25, 2004. doi: 10.1002/0470091355.ecm009. URL `https://onlinelibrary.wiley.com/doi/pdf/10.1002/0470091355.ecm009`.

Lawrence C. Evans. *Partial Differential Equations*. American Mathematical Society, 1998. ISBN 0-8218-0772-2.

Lawrence C. Evans. Entropy and Partial Differential Equations. Lecture notes, 2018. URL `https://math.berkeley.edu/~evans/entropy.and.PDE.pdf`.

Kolumban Hutter and Klaus Jöhnk. *Continuum Methods of Physical Modeling*. Gardners Books, 2010. ISBN 978-3-642-05831-8.

Mika Juntunen and Rolf Stenberg. Nitsche's method for general boundary conditions. *Mathematics of Computation*, 78(267):1353–1374, Jan 2009. doi: 10.1090/s0025-5718-08-02183-2.

Mark Kachanov, Boris Shafiro, and Igor Tsukrov. *Handbook of elasticity solutions*. Kluwer Academic Publishers, 2010.

Boris J.p. Kaus, Hans Mühlhaus, and Dave A. May. A stabilization algorithm for geodynamic numerical simulations with a free surface. *Physics of the Earth and Planetary Interiors*, 181(1-2):12–20, 2010. doi: 10.1016/j.pepi.2010.04.007.

Zdeněk Martinec. Continuum Mechanics. Lecture notes, 2003. URL `http://geo.mff.cuni.cz/vyuka/Martinec-ContinuumMechanics.pdf`.

Ctirad Matyska. Mathematical Introduction to Geothermics and Geodynamics. Lecture notes, 2005. URL `http://geo.mff.cuni.cz/users/matyska/geoterm.pdf`.

Guglielmo Scovazzi and Thomas J. R. Hughes. Lecture notes on continuum mechanics on arbitrary moving domains. Lecture notes, Jan 2007.

John R. Spencer and Francis Nimmo. Enceladus: An Active Ice World in the Saturn System. *Annual Review of Earth and Planetary Sciences*, 41(1):693–717, 2013. doi: 10.1146/annurev-earth-050212-124025.

List of Figures

List of Tables

Attachments

A Appendix A: Notation

Throughout the thesis we employ the Einstain summation convention and use mostly cartesian coordinates, therefore we do not make difference between covariant and contravariant bases. Preferably, we use the operator notation meaning contraction over the rightmost index, i.e.:

$$\mathbb{A}\mathbf{u} \coloneqq A_{ij}u_j\mathbf{e}_i,$$
$$\operatorname{div}\mathbb{A} \coloneqq \frac{\partial}{\partial x_j}A_{ij}\mathbf{e}_i.$$

Other notation definitions:

$$\mathbb{A} : \mathbb{B} \coloneqq A_{ij}B_{ij},$$
$$\nabla\mathbf{a} \coloneqq \frac{\partial a_i}{\partial x_j}\mathbf{e}_i \otimes \mathbf{e}_j.$$

B Appendix B: Some differential operators in curvilinear coordinates

Consider a vector function $\mathbf{a} = a_r\mathbf{e}_{\hat{r}} + a_\varphi\mathbf{e}_{\hat{\varphi}} + a_z\mathbf{e}_{\hat{z}}$ in cylindrical coordinates, or $\mathbf{a} = a_r\mathbf{e}_{\hat{r}} + a_\varphi\mathbf{e}_{\hat{\varphi}} + a_\vartheta\mathbf{e}_{\hat{\vartheta}}$ in spherical coordinates and assume that f is a scalar function. Following Table 2 offers an overview of some differential operators in cylindrical and spherical coordinates.

Differential operator	**Cylindrical coordinates** (r, φ, z)	**Spherical coordinates** (r, φ, ϑ)
∇f	$\frac{\partial f}{\partial r}\mathbf{e}_{\hat{r}} + \frac{1}{r}\frac{\partial f}{\partial \varphi}\mathbf{e}_{\hat{\varphi}} + \frac{\partial f}{\partial z}\mathbf{e}_{\hat{z}}$	$\frac{\partial f}{\partial r}\mathbf{e}_{\hat{r}} + \frac{1}{r}\frac{\partial f}{\partial \varphi}\mathbf{e}_{\hat{\varphi}} + \frac{1}{r\sin\varphi}\frac{\partial f}{\partial \vartheta}\mathbf{e}_{\hat{\vartheta}}$
$\operatorname{div}\mathbf{a}$	$\frac{1}{r}\frac{\partial (ra_r)}{\partial r} + \frac{1}{r}\frac{\partial a_\varphi}{\partial \varphi} + \frac{\partial a_z}{\partial z}$	$\frac{1}{r^2}\frac{\partial (r^2 a_r)}{\partial r} + \frac{1}{r\sin\varphi}\frac{\partial (a_\varphi \sin\varphi)}{\partial \varphi} + \frac{1}{r\sin\varphi}\frac{\partial a_\vartheta}{\partial \vartheta}$
Δf	$\frac{1}{r}\frac{\partial}{\partial r}\left(r\frac{\partial f}{\partial r}\right) + \frac{1}{r^2}\frac{\partial^2 f}{\partial \varphi^2} + \frac{\partial^2 f}{\partial z^2}$	$\frac{1}{r^2}\frac{\partial}{\partial r}\left(r^2\frac{\partial f}{\partial r}\right) + \frac{1}{r^2\sin\varphi}\frac{\partial}{\partial \varphi}\left(\sin\varphi\frac{\partial f}{\partial \varphi}\right) + + \frac{1}{r^2\sin^2\varphi}\frac{\partial^2 f}{\partial \vartheta^2}$

Table 2: Differential operators in curvilinear coordinates, taken from appendix of [Kachanov et al., 2010].